EVALUATION OF MOISTURE DIFFUSIVITY IN COPRA AT DIFFERENT DRYING CONDITIONS

Agampodi Radeesha Laknath Mendis

(158033M)

Degree of Master of Science

Department of Chemical and Process Engineering

University of Moratuwa

Sri Lanka

December 2017

EVALUATION OF MOISTURE DIFFUSIVITY IN COPRA AT DIFFERENT DRYING CONDITIONS

A.R.L.Mendis

(158033M)

Thesis/Dissertation submitted in partial fulfillment of the requirements for the degree Master of Science

Department of Chemical and Process Engineering

University of Moratuwa

Sri Lanka

December 2017

Declaration

I declare that this is my own work and this thesis/dissertation does not incorporate without acknowledgement any material previously submitted for a Degree or Diploma in any University or other institute of higher learning and to the best of my knowledge and belief it does not contain any material previously published or written by another person except where the acknowledgement is made in the text"

Signature:…… Date:…….

Copyright Statement

I hereby grant the University of Moratuwa the right to archive and to make available my thesis or dissertation in whole or part in the University Libraries in all forms of media, subject to the provisions of the current copyright act of Sri Lanka. I retrain all proprietary rights, such as patent rights. I also retain the right to use in future works (such as articles or books) all or part of this thesis or dissertation.

Signature:…… Date:…….

I have supervised and accepted this thesis/dissertation for the award of the degree

Signature of the Supervisor:……. Date:…….

Dr. A.D.U.S. Amarasinghe
Senior Lecturer
Department of Chemical and Process Engineering
University of Moratuwa

Signature of the Co- Supervisor:……Date:…….

Dr. M. Narayana
Senior Lecturer
Department of Chemical and Process Engineering
University of Moratuwa

Abstract

Copra is one of the major traditional products processed from coconuts and is used primarily as a source of coconut oil. It is the kernel of coconut after reducing the moisture content from about 50% (dry basis) to about 6% (dry basis) by drying. Traditional drying processes are vastly used in manufacturing of copra and that has created many quality problems leading to hygienic and health issues which can be minimized by using controlled drying techniques. Controlled drying is also a primary requirement in producing edible copra and premium products like virgin coconut oil.

Accurate prediction of moisture diffusivity of porous materials like food under given conditions is important in analysing the drying process. In this study drying behaviour of copra was examined and two methods were suggested to predict the moisture diffusivity of copra. In the first method, the moisture diffusivity of copra was determined for the first and second falling rate periods. A critical moisture content of 30% (dry basis) was identified as the probable limit between the first and second falling rate periods. A computational fluid dynamic model was used to fine-tune the system parameters with experimental data and the effective moisture diffusivity values at 55 ºC for first and second falling rate periods were found to be 1.10×10^{-8} and 1.99×10^{-9} m^2s^{-1} respectively.

In the second method, moisture diffusivity of copra was found as a function of drying temperature and dry basis moisture content. Drying experiments were performed for seven different temperatures in the range of 45 – 75 ºC to obtain drying curves of copra. The moisture diffusivity was found to be an exponential function of moisture content where the model parameters were linearly varied with temperature. Further the volume shrinkage of copra was linearly correlated with moisture content. A three-dimensional numerical model was developed to predict the spatial distribution of moisture inside the copra using computational fluid dynamics (CFD) with OpenFOAM software. Results of the spatial moisture distribution were graphically presented. The results of simulation were in agreement with the experimental observations and the optimum temperature for drying of copra was found to be about 60 ºC for 20 hours of drying time.

Keywords: Copra drying, Moisture diffusivity, Numerical simulation

Acknowledgement

Completion of this thesis has been one of the most significant academic challenges I have ever had encounter. Without the support, patience and guidance of the following people, this task would not have been accomplished. It is to them that I owe my deepest gratitude.

I am really thankful to my main supervisor Dr.A.D.U.S.Amarasinghe and co-supervisor Dr.M.Narayana for giving me their fullest support from the beginning. Their advices and guidance were always helpful to me to complete this study. I am grateful to Dr P.G.Rathnasiri former Head of the Department of Chemical and Process Engineering for giving me the opportunity to do the M.Sc in the department. This research work was supported by University of Moratuwa Senate Research Grant Number SRC/LT/2015/10 and it was great financial encouragement for my research work.

I would like to express my deep gratitude to Mrs. Poorasinghe (Director Quality Assurance division of CDA) and Mr Ashoka Pushpakumara (Assistant Director Quality Assurance division of CDA) for giving me required information on the field of study.

Next, I must mention that support I received from my friends. Mr. Niranjan Fernando and Mr.Kasun Udana supported me much on finding required information in my research area. Mr. Kasun Anuranga, Ms Imalsha Abaysooriya, Mr. M. H. K. Chithalka, Mr. S. L. M. Mudalige, Mr. Kasun Samarasiri and Mr. Charith Bandara helped me much during experimental works. I place on record my sense of gratitude to them for their tremendous support which has offered me great convenience during my works.

I wish to express my thanks to the laboratory staff of Department of Chemical and Process Engineering, University of Moratuwa for their helps during my lab works. I would like to convey special thanks to the technical officers, Mr. Jayaweera and Miss. Dinooshi for their assistance during laboratory works.

Last but not least I wish to avail myself of this opportunity, express a sense of gratitude and love to my beloved parents and sisters for their manual support, strength, helps and for everything throughout my life.

Contents

List of Figures

List of Tables

Nomenclature

$C_{p,a}$	*Specific heat capacity of air*
D_{bin}	*water vapor diffusivity in dry air*
D_w	*Diffusion coefficient of water*
h_t	*Convective heat transfer coefficient*
I	*Evaporation rate*
J	*Volume shrinkage*
k_a	*Thermal Conductivity of air*
K_{evp}	*Evaporation rate constant*
K_m	*Convective mass transfer coefficient*
k_v	*Thermal Conductivity of vapor*
L	*Characteristic length*
n	*flux*
P	*Atmospheric pressure*
P_r	*Prandtl number*
P_{sat}	*Saturation vapor pressure*
R_e	*Reynolds number*
r	*Drying rate*
t	*time*
T_s	*Absolute temperature of solid phase*
U_a	*Velocity of air*
U_w	*Velocity of water*
V_0	*Initial volume*
V_t	*Volume at time t*
X	*Moisture content (%(w/w) Dry basis)*
X_e	*Equilibrium Moisture Content*
X_g	*Gas phase moisture*
X_0	*Initial Moisture Content (%(w/w) Dry basis)*
Greek letters	
ρ_a	*Density of air*
ρ_{amb}	*Ambient vapor density*
ρ_v	*Density of vapor*
$\rho_{v,eq}$	*Equilibrium vapor density*
ρ_w	*Density of water*
φ	*Porosity-function of moisture*
μ	*Viscosity of water*

1. Introduction

1.1 Copra drying

Copra is the primary product which is manufactured by drying of coconut kernel. It is largely used in food industry while using in many non-food applications like pharmaceuticals and cosmetics [1]. Copra can be mainly considered as an intermediate output of the coconut oil manufacturing process because a major portion of world's copra production is utilized for coconut oil production. The copra made for coconut oil production is called as "Milling copra". Copra is also produced as "edible copra" to fulfil the demand of consuming directly as food but the quantity is much less than milling copra. The oil can be extracted from either wet or dry coconut kernel and the process is named as dry process or wet process accordingly. Dry processing with mechanical expellers is the widely used extracting method of oil in most of the countries [2]. Virgin oil is a distinctive quality extracted coconut oil using the standard level of copra by using only the physical methods. Sri Lanka is now looking for the development of value added items but still depends on the traditional export items like coconut. Virgin coconut oil is the latest high value product of coconut very much required next to its human nutraceutical return and as a utilitarian food. The demand for virgin oil and eatable copra is highly related on the quality of copra. The final moisture content of copra should be decreased to about 7% for producing good standard coconut oil [3]. The high moisture content provides an ideal medium for bacteria and fungi. This leads to creation of Aflatoxin which is a cancer causing toxic substance. The low quality copra always results in producing bad quality coconut oil. High moisture content of copra also causes higher free fatty acid levels in the oil and these free fatty acids cause rancidity in oil with bad odour.

Direct contact of copra with smoke and burnt gases in kiln drying process cause deposition of polycyclic aromatic hydrocarbons (PAH) on the kernel of copra [4]. Presence of Aflatoxin and PAH in copra can be transferred to the coconut oil during the extraction process [5]. In addition, coconut oil colour is strongly affected by colour of copra. Copra become brown due to direct contact of smoke in kiln drying and brown copra gives brown coconut oil. In Sri Lanka, majority of copra is manufactured by kiln drying and the standard of copra differs with the skill of

operator and climatic conditions [4]. Indirect hot air drying is a better alternative for kiln drying. It can produce good quality copra since it avoids smoke deposition and colour of the copra is mostly white or light brown [6], [7].

Even if high temperature increases the rate of drying, it produces brown copra and causes case hardening of copra. Case hardening is the formation of a hard outer layer on coconut kernel which limits the way of moisture movement from the interior to the shallow [7]. The highest temperature for drying copra without deteriorating the quality was found to be in the range of 60 – 70 °C. Thanaraj, Dharmasena, & Samarajeewa, (2004) suggested an optimum temperature of 60°C while Mohanraj, & Chandrasekar, (2008a) reported the highest drying temperature of 63°C [7], [8]. Relative humidity of air and the velocity of air also affect the drying speed of copra but the effect is not as considerable as temperature [9].

1.2 Numerical simulation of drying

The simulation based mathematical models minimize the cost, time requirement and any potential risks that may be present in actual experimental analysis. Mathematical models can produce a large number of data points as compared to fewer experimental data. Spatial distributions of variables within the food materials can be analyzed using these models. With the recent developments in the computer hardware, computational fluid dynamics (CFD) is widely applied as a numerical modeling tool. Transport of moisture within porous structures was analyzed using CFD simulations for food materials such as potato chips, apple cubes and quince slices. In most of these studies moisture diffusivity was used as constant or as simple functions of moisture content and temperature [10], [11], [12]. However, moisture diffusivity is a system specific and complicated function [13], [14]. Therefore it is essential to understand the functional behaviour of moisture diffusivity in terms of other common parameters such as temperature for the simulation and optimization of the drying processes. For food materials, liquid diffusion can be identified as the main mechanism of moisture transport within the first falling rate period. Whereas the vapor diffusion dominates within the second falling rate period. Drying of most of the food materials was found to occur during the falling rate periods with the absence of constant rate period [15], [16], [17].

1.3 Objectives

The scope of the present work was to determine the diffusivity of moisture and to predict the spatial distribution of moisture in copra during hot air drying.

The objectives of the study are

1) Determine the moisture diffusivity of copra for the first and second falling rate periods
2) Develop a diffusivity model with respect to external parameters by considering heat and mass transfer during drying and shrinkage of copra
3) Describe the spatial distribution of moisture inside copra by analysing the moisture transport within the porous structure and also considering shrinkage of copra during hot air drying

1.4 Outline of the thesis

This thesis is consisted with eight chapters. In the first chapter, the research project is introduced and the research objectives are given. A literature review on production, applications, methods of drying, quality standards of copra and numerical simulation in drying process has been presented in the second chapter. Third and fourth chapters describe the model development with derivations of equations and numerical simulation with OpenFOAM software. In the fifth chapter, materials used, experimental procedure and the methodology followed to fulfil the research objectives are described. The results obtained during the current study are presented and discussed in chapters six and seven. The last and eighth chapter summarizes the conclusions of the study.

2. Literature Review

2.1 Copra

2.1.1 Production and applications

The coconut tree is mostly known as the tree of life because coconut tree provides all the necessities of life. Coconut tree has bound with Sri Lankan life style since thousands of years ago. Many historical stories can be found about the history of coconut tree in Sri Lankan folklore. The development of coconut cultivation which was started in king's era continued to even in the colonial era. Later, the Sri Lankan governments contributed towards coconut cultivation by many ways. At present, three institutions have been established for developing coconut industry namely Coconut Cultivation Board, Coconut Research Institute and Coconut Development Authority.

Few industries have been developed in relation to the coconut tree which can be categorized into four main types namely products related to fruit, products related to coconut flower, products related to coconut trunk and the products related to coconut leaves. Products related to fruit come with three main sources namely coconut kernel, coconut husk and coconut shell [18]. Copra is a primary product which is produced by drying of coconut kernel. The name copra has been derived from the Malayalam word kopra for dried coconut. The drying operation reduces the moisture content in the kernels from about 50% to 6%.

Several methods have been developed for copra making throughout the world. Among them, kiln drying is the widely used method while sun drying and hot air drying are also practiced. In 1923, an indirectly heated air dryer called "Chula Dryer" was introduced in Sri Lanka for manufacturing copra. "Ceylon Copra Kiln" which was designed by Coconut Research Institute was introduced in 1960s. This dryer was a direct air heated dryer and was more economical than the previous dryer [4]. Therefore, Ceylon copra kiln has been using vastly not only in large scale commercial copra manufacturing mills but also some small scale copra manufacturers since 1960 with several developments in time to time. In addition to this, sun during of copra can still be seen in rural areas at domestic level. Most of the

copra mills are situated in coconut triangle area and in the coastal area from Negombo to Tangalle [18].

Coconut oil is the oil contained in the coconut kernel. It has been consumed in tropical countries including Sri Lanka since many centuries mainly as edible oil. Two main oil extraction processes are used in industrial scale operations which are categorized as dry process and wet process according to the form of kernel. Dry process is the traditional oil extraction process which uses copra. In the wet process, oil is extracted using fresh kernel [19]. In Sri Lanka, dry process is the most popular method and at present more than 250 oil mills are registered with CDA (Coconut Development Authority). Many of these oil mills are also situated within the coconut triangle while few are in coastal area from Negombo to Tangalle. In some mills, production of both copra and coconut oil is done at the same place. The size of the kiln depends on the capacity of the mill.

Coconut oil is used heavily in the food industry. In Sri Lanka, it has been extensively used as cooking oil from the day of its origin. It also has some applications in medical and pharmaceutical industries. A very common application of coconut oil is soap and detergent industry and the other applications include glycerol manufacturing, cosmetic industry, plastic industry, rubber industry, etc. At present, it is being tested for using as biofuel.

2.1.2 Quality standards and testing

Copra is the dried kernel of coconuts. Generally, fresh coconut kernel contains approximately 50 % (w/w wet basis) moisture. Ideally, the coconut kernel should be dried till the moisture content reached the equilibrium moisture content of copra to store them safely. Typically, the equilibrium moisture content for copra is around 6% to 7% in hot countries. Therefore, well dried copra contains moisture around 6% to 7%. The high moisture content and existence of protein and sugar makes the renewed coconut kernel an ideal medium for the growth of bacteria and fungi. But at a moisture content around 6%, mold growth in copra is inhibited [19]. Improper drying and storage result in more free fatty acid, more moisture, low color, unpleasant odor, more amount of singed copra, molding, and dirt integration, resulting in lower grade copra [20].

Drying of copra into a safer moisture level is always a vital requirement because higher moisture contents of copra support the formation of Aflatoxin in copra [5]. Aflatoxins are toxic chemicals commonly found in groundnut and maize. But Aflatoxin contamination is comparatively at a lower level in copra. The risk of Aflatoxin contamination in copra increases with the moisture content and the safe moisture level for hot-air dried copra was found to be 8%. Since the smoke particles inhibit the mould growth, the tolerable limit for the smoke desiccated copra is at a relatively higher level of 11% according to a recent study carried out in Philippines by the Natural Resources Institute of UK [5].

There are four main types of Aflatoxins namely B1, B2, G1, and G2, and Aflatoxin B1 is the generous type. It is carcinogenic and found to cause liver cancer in all the tested animals. According to previous studies, a mean level of 50 ppb of Aflatoxin B1 was recorded from the coconut oil samples collected during rainy and hot seasons in Sri Lanka [21]. The same study, also recorded detection of a mean level of 186 ppb of Aflatoxin B1 in the coconut oil manufactured in lower level oil mills. Therefore, the reduction of the moisture content of copra is important to avoid health hazards related with Aflatoxin.

Moisture content and appearance are the main quality parameters for copra [22]. Copra with acceptable moisture content of less than 7% and the pale white to light brown colours fetch higher prices in the international markets. The appearance is also important as scorched, burned, sooty and mouldy copra have less demand. Since copra is mainly used for the production of coconut oil, the quality of copra directly affects the quality of coconut oil. The existing quality parameters for coconut oil were adopted from the 1990 guidelines published by the Federation of Oils, Seeds and Fats Association (FOSFA). According FOSFA guidelines, the maximum allowable fatty acid level is 4% and the acceptable colour is on the Lovibond range of lower than 9 red and 50 yellow [5].

2.1.3 Copra drying process

Rate of Copra drying depends on number of factors. They are related to environmental conditions, physical properties of copra, the drying principles used and physical properties of the drying air (humidity, temperature and velocity).

Among all of these factors, the rate of drying depends mainly on the temperature of the drying air. Thus, several studies have been carried out to find the optimum temperature for drying copra. Krishna Raghavan (2010) described that high drying air temperatures will increase the rate of drying, but at the expense of quality. He recommended a two-stage drying process with initial drying at high temperature followed by a period of lower temperature drying. Drying copra at high temperatures for a long time may cause case hardening. Case hardening refers to the formation of a hard outer layer which restricts the passage of moisture movement from the interior to the surface [5]. Satter, M. A. (2003) also recommended to maintain three different temperature levels High (70 – 85 ºC), Medium (55 – 70 ºC) and Low (40 – 55 ºC) [23]. Thiruchelwam Thanaraj, et al (2007) described the importance of maintaining an optimum temperature of 60 ºC to avoid case hardening and burnt patches due to high temperatures and to avoid mould growth and extended drying time due to lower temperatures [6]. Roberto, C. Guoarte, et al (1996) used much higher temperatures (90 ºC) than the others but they failed to produce white copra [5].

Relative humidity of air also affects the drying rate of copra but the effect is not as considerable as temperature. The effect of air velocity on drying was also discussed by many researches. Roberto, C. Guoarte, et al (1996) recommended an air velocity of 0.5 ms^{-1} for industrial scale copra drying while Mohanraj, M. and Chandrasekar, P. (2008) reported that the optimum velocity for copra drying was 1.2 ms^{-1}[3], [5]. But, according to Satter, M. A. (2003) air velocity has the least effect on drying as the moisture within the kernel takes relatively long time to reach the surface before being picked up by unsaturated hot air [23].

Several methods are used for drying copra throughout the world. Those can be categorized into three main types: natural drying, smoke drying, hot air drying. Natural drying involves the use of direct heat from sun in open areas. It is the simplest and cheapest method, but is heavily dependent on climatic conditions. Sun drying takes about 7 days to reduce the moisture content of copra to around 10%.

However, if rains during this period, copra may contaminate with fungi and produce a grey rancid product. Furthermore, sun drying requires more space, is labour intensive and there can be deteriorations in quality in open sun drying from deposits of dirt and dust [3]. On the other hand, sun drying produces more white copra than direct dryers and it is more suitable for small holders who are living in the areas with high solar radiation and having long sunny days [6].

The smoke drying involves the use of traditional fuels such as firewood, copra husks and shells. The copra bed is placed on a wire mesh directly above the heat source. The combustion products pass through the copra bed, and remove the free moisture on the copra surface. Although the efficiency of drying is considerably higher than that of natural drying, this method leads to poor quality copra due to bad color and scorching. Some advantages of these dryers are higher thermal efficiency, low cost of construction and fuel and simplicity of design [24].

In the hot air drying hot air flow is generated from a hot air blower through the copra bed. This method is more efficient with reduced drying time cycle. The main advantage of hot air dryers is their ability to produce high quality, clean and white copra without PAH problems. It is the most expensive drying method with a relatively large initial capital. This type of dryers is hard to find in large scale copra drying. The operating cost of air circulation equipment has been a concern for rural farmers and that has made low popularity of these forced draft dryers.

2.2 Drying characteristic of porous materials

The drying characteristic of porous materials such as fruit and vegetable products was extensively reported in the past [25], [26], [27]. Drying process can be explained by the two main regions; constant rate period and falling rate periods. Sometimes more falling rate periods, which is mainly depends on material characteristics such as porosity and shrinkage during drying, are observed [28], [29].

Drying in the constant rate period is governed by external factors such as the temperature difference between the hot air and the drying surface, surface area of the material and the heat and mass transfer coefficients. It can be assumed that the moisture removal by evaporation is constant during the falling rate period as the

internal moisture transfer is sufficient enough to maintain the surface at saturated conditions [25], [30].

The moisture content at the transition from the constant rate period to the first falling rate period is defined as the critical moisture content. For fruits and vegetables critical moisture content was found to be similar to initial moisture content and the constant rate period is not noticeable for some of fruits and vegetables such as avocado and tapioca. Moreover drying behaviour of most of the biological materials can be described only by falling-rate periods [26], [31], [32] [33]. The falling rate period is an internally controlled mechanism where the interior transport of moisture is less than the rate of evaporation from the surface. Internal resistance to transport of moisture gradually increases during the first falling rate period and becomes critical at the beginning of the second falling rate period where the partial pressure of water within the entire material reach below the saturation level [25]. Therefore the removal of the last 10% of the moisture is the most difficult and it takes equivalent time to the removal of first 90% of moisture. Equilibrium moisture content is achieved as the vapor pressure of the material becomes equal to the partial vapor pressure of the hot air and no further drying is taken place at this stage [28].

2.3 Numerical simulation of Drying

2.3.1 Analysing the drying process

Drying is an essential operation in the chemical, agricultural, biotechnology, food, polymer, ceramics, pharmaceutical, pulp and paper, mineral processing, and wood processing industries because drying extends product stability (prevention of growth and reproduction of undesirable microorganisms), enhances product quality (minimization of moisture mediated deterioration reactions, e.g. nutrient loss, product discoloration), and provide ease of handling the product (reduction in product weight and volume, decreased packing, storage and transportation costs) [34].

Drying is the process of thermally removing moisture from a moist material by evaporation. Moisture held in moist food material as loose chemical combination, present as a liquid solution or trapped in the microstructure of the food material, which exerts a vapor pressure less than that of pure liquid is called bound moisture.

Moisture in excess of bound moisture is called unbound moisture. Drying involves two processes to occur simultaneously, one is transfer of heat from the surrounding environment to evaporate the surface moisture and second is transfer of internal moisture to the surface of the food material and its evaporation due to process one. In first process, the removal of water as vapor from the material surface depends on the external conditions like air temperature, humidity, velocity, area of exposed surface, and pressure. In second process, the movement of moisture internally within the food material is a function of the physical nature of the food material, the temperature, and its moisture content. Drying rate depends on the rates of two processes mentioned above. Transport of moisture within the food material may occur by any one or more of the following mechanisms of mass transfer [35]; liquid diffusion (if the moist food material is at a temperature below the boiling point of the liquid), vapor diffusion (if the liquid vaporizes within material), Knudsen diffusion (if drying takes place at very low temperatures and pressures), hydrostatic pressure differences (when internal vaporization rates exceed the rate of vapor transport through the solid to the surroundings) or combinations of the above mechanisms.

2.3.2 Numerical modelling of drying process

There has been a large amount of numerical work with varying degrees of complexities for prediction of drying rate of food products. The majority of the models which are available in the literature consider only mass transfer (no heat transfer) assuming that the drying occurs almost isothermally or the gradient of the temperature around the food material is too small to have any effect in the mass transfer process [36], [37], [38].

Several experimental studies were reported on evaluating the drying rates and total drying time at different drying conditions for porous materials [39], [40], [41], [42]. However, the experimental analysis of spatial distribution of moisture and/or temperature within the porous structure was found to be a tedious task due to the requirement of advanced radiography or tomography methods for measurement [43], [44]. However, mathematical and numerical models have been successfully used in the recent past to explain the spatial variation of parameters within the biological material. These models were manly based on two approaches using; Darcy equation

to describe the capillary action and Fick's Law to describe the moisture diffusion in the material [45], [46], [47].

Wang and Brennan developed a 1-D mathematical model of simultaneous heat and moisture transfer for the prediction of moisture and temperature distributions during drying in a slab-shaped solid [43]. The model was applied to the air drying of potatoes. They concluded that shrinkage had an influence on the drying behaviour of potato and should be taken into account in predictive models. In a separate study a1D model was proposed with consideration of evaporation at the surface [48] and semi-analytical solutions were presented for carrot slabs with the effect of Biot number and relative humidity. All these studies considered a constant convective coefficient at the boundaries. Most of these analyses are for a lower air velocity range of 0.1-0.3 m/s with an assumption of laminar flow [49].

2.3.3 Determination of moisture diffusivity in food materials

Diffusion is the process of transport of mass due to concentration difference between one part of the system and another. It leads to reach the equilibrium moisture contents within the porous media with time [50]. This has been used extensively in explaining the physical mechanism of moisture transport of dehydration of food materials [51]. Specifically the moisture loss during the falling rate period could be explained reasonably well by applying the Fick's second law of diffusion [52], [53]. The experimental results were found to be in good agreement with the predicted data for drying rate and drying time but the application of Fick's second law in predicting the moisture distributions within the materials was limited [54], [55], [56]. Further, when the system becomes more complex, the experimental data were found to deviate from the predicted [57]. Therefore more complex solutions are required incorporating the heat transfer equations in addition to mass transfer equations.

Effective moisture diffusivity for various food and agricultural materials were estimated using experimental drying curves and more than 1700 data have been published since 1975 [58]. In most of these studies, the simplified assumption of constant diffusion coefficient was used and one-dimensional diffusion was modeled for known geometries such as sphere, cylinder and slab. Further the initial moisture

content was assumed to be uniformly distributed. The temperature gradient and shrinkage was also assumed to be negligible during drying.

The effective diffusivity varies with the moisture content and also the drying temperature [53], [55], [60]. The temperature dependence of the moisture diffusivity of food materials could be described by an Arrhenius relationship [29], [33], [60], [61], [62]. The diffusion theory was found to fail at very low moisture contents [59]. This may be mainly attributed to the variation of effective moisture diffusivity during drying. During the second falling-rate period of drying, the moisture diffusivity of various foods was found to be about four to eight times lower than those in the first falling-rate period [25], [28].

Shrinkage has a major impact on the drying process of food materials and it can be identified as a main factor for the variation of moisture diffusivity during drying. Consequently, the use of Fick's second law becomes restricted in measuring the diffusion coefficient. In order to overcome this problem, Crank (1975) suggested a one-dimensional volume change while Fish (1954) suggested a three-dimensional isotropic volume change [63], [64]. However, the concept of arbitrary volume change suggested by Lambert (1991) described the real volume change more effectively [65].

Shrinkage also affects the physical properties such as porosity and density of biological materials and hence it is important to have a good knowledge on shrinkage phenomenon for the better control of drying process of such materials [66]. Although moisture diffusivity of some materials could be predicted with the assumption of constant moisture diffusivity, the validity was found to be limited to a narrow range of moisture [43], [67]. Simal (1998) predicted the drying curves by considering the shrinkage effect and ignoring it and concluded that the model with shrinkage effect predicted the drying process comparatively better than the model without shrinkage effect [68], [69].

2.4 Justification

The demand of the coconut oil is mainly depends on the quality of copra which is the major raw material of coconut oil. Therefore, understanding of moisture transport inside the copra is a vital requirement to control the hot air drying process to make good quality copra. This can be done by numerical simulation of hot air drying using

computational fluid dynamics. Accurate prediction of moisture diffusivity of porous materials like food under given conditions is important for analysing the drying process. Many research works have been done in the past to determine moisture diffusivity of various foodstuffs mainly potatoes using various experimental and analytical methods [36], [70], [71], [72]. However, the analytical solutions rely mostly on two very restrictive hypotheses; constant moisture diffusivity and constant volume of the product. The numerical modelling and simulations enables the analysis of the drying process with variation of the product volume and the moisture diffusivity with time. Several numerical modelling and simulation works reported on drying of food materials were based on constant moisture diffusivity and one dimensional moisture transfer and material shrinkage [11], [12], [38], [43]. The present work determines the diffusivity of moisture in copra during hot air drying as a function of moisture content and temperature. A numerical model has been developed to describe the spatial distribution of moisture inside copra by analysing the moisture transport within the porous structure and also considering shrinkage of copra during hot air drying.

3. Model Development

3.1 Governing Equations

Numerical model was developed by considering mass balance to obtain the spatial distribution of moisture inside the copra. These equations are called the governing transport equations. The governing transport equation for a general scalar quantity ∅ is obtained by considering the conservation of ∅ over a differential volume element of the solution domain. The differential form of general transport equation for the general variable ∅ is shown in equation (3.1).

$$\frac{\partial \emptyset}{\partial t} + div(\rho \emptyset u) = div(\tau grad \emptyset) + I \qquad (3.1)$$

Where

I - Rate of φ due to sources (evaporation rate)

$\frac{\partial \emptyset}{\partial t}$ - Rate of increase of φ of fluid Element

$div(\rho \emptyset u)$ - Net rate of flow of φ out of fluid element

$div(\tau grad \emptyset)$ - Rate of increase of φ due to diffusion

3.1.1 Momentum conservation equation

The momentum conservation equation is derived by applying the momentum balance in each coordinate direction to the differential volume element. Figure 3.1 shows the fluxes of x momentum. Note that $\emptyset_{ij}$ is the combined momentum flux tensor which can be interpreted as the flux of *j* momentum in *i* direction.

The momentum balance can be written as [73],

$$\left\{\begin{matrix}\text{Rate of increase} \\ \text{of momentum}\end{matrix}\right\} = \left\{\begin{matrix}\text{rate of} \\ \text{momentum in}\end{matrix}\right\} - \left\{\begin{matrix}\text{rate of} \\ \text{momentum out}\end{matrix}\right\} + \left\{\begin{matrix}\text{external} \\ \text{force}\end{matrix}\right\}$$

The total rate of x momentum into the fluid element can be written as,

$$(\emptyset_{xx})|_x \Delta y \Delta z + (\emptyset_{yx})|_y \Delta x \Delta z + (\emptyset_{xz})|_z \Delta x \Delta y$$

And the total rate of x momentum out of the system is equal to,

$$(\emptyset_{xx})|_{x+\Delta x} \Delta y \Delta z + (\emptyset_{yx})|_{y+\Delta y} \Delta x \Delta z + (\emptyset_{xz})|_{z+\Delta z} \Delta x \Delta y$$

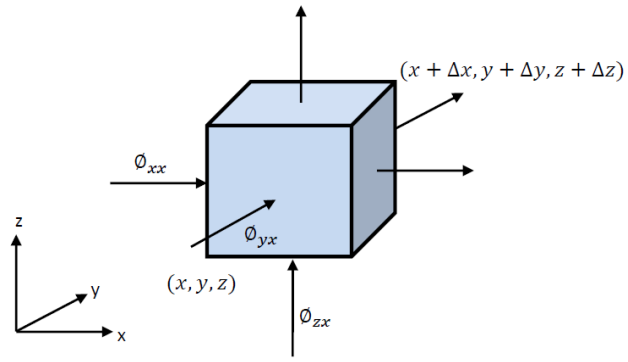

Figure 3.1 Differential volume element located in flow domain and x momentum fluxes across its faces

The external gravitational force on the fluid element in *x* direction is given by,

$$\rho g_x \Delta x \Delta y \Delta z$$

Substituting these expressions in the momentum balance relation results in,

$$\Delta x\Delta y\Delta z\frac{\partial}{\partial t}\rho U_x = \Delta y\Delta z\left((\emptyset_{xx})|_x - (\emptyset_{xx})|_{x+\Delta x}\right) + \Delta x\Delta z\left((\emptyset_{yx})|_y - (\emptyset_{yx})|_{y+\Delta y}\right) + \Delta x\Delta y\left((\emptyset_{zx})|_z - (\emptyset_{zx})|_{z+\Delta z}\right) + \rho g_x\Delta x\Delta y\Delta z \quad (3.2)$$

Dividing the entire equation by *Δx Δy Δz* and rearranging,

$$\frac{\partial}{\partial t}\rho U_x = -\frac{(\emptyset_{xx})|_{x+\Delta x}-(\emptyset_{xx})|_x}{\Delta x} - \frac{(\emptyset_{yx})|_{y+\Delta y}-(\emptyset_{yx})|_y}{\Delta y} - \frac{(\emptyset_{zx})|_{z+\Delta z}-(\emptyset_{zx})|_z}{\Delta z} + \rho g_x \quad (3.3)$$

Taking the limit as *Δx, Δy* and *Δz* go to zero, results in the following partial differential equation for the *x* component of velocity,

$$\frac{\partial}{\partial t}\rho U_x = \left(\frac{\partial}{\partial x}\emptyset_{xx} + \frac{\partial}{\partial y}\emptyset_{yx} + \frac{\partial}{\partial z}\emptyset_{zx}\right) + \rho g_x \quad (3.4)$$

By similarly considering the fluxes in other directions, equations for *y* and *z* momentum can be derived as expressed below.

$$\frac{\partial}{\partial t}\rho U_y = \left(\frac{\partial}{\partial x}\emptyset_{xy} + \frac{\partial}{\partial y}\emptyset_{yy} + \frac{\partial}{\partial z}\emptyset_{zy}\right) + \rho g_y \quad (3.5)$$

$$\frac{\partial}{\partial t}\rho U_z = \left(\frac{\partial}{\partial x}\emptyset_{xz} + \frac{\partial}{\partial y}\emptyset_{yz} + \frac{\partial}{\partial z}\emptyset_{zz}\right) + \rho g_z \quad (3.6)$$

For a general coordinate direction *i*, these equations can be written as

$$\frac{\partial}{\partial t}\rho U_i = -[\nabla.\emptyset]_i + \rho g_i \quad (3.7)$$

Where $\nabla.\emptyset$ represents the contraction of the second order momentum flux tensor with the differential operator $\frac{\partial}{\partial x^i}$

Combining the separate equations for each coordinate direction, the final vector form of the momentum equation can be written as,

$$\frac{\partial}{\partial t}\rho \boldsymbol{U} = -[\boldsymbol{\nabla}.\emptyset] + \rho \boldsymbol{g} \qquad (3.8)$$

The combined momentum flux tensor $\emptyset$ is given by,

$$\emptyset = \rho U \otimes U + p\delta + \tau \qquad (3.9)$$

Where δ is the kroneker delta symbol and τ is the molecular momentum flux tensor. For a Newtonian fluid, τ is given by Newton's law of viscosity,

$$\tau = -\mu \nabla U \qquad (3.10)$$

Substituting these relations into equation (3.8), results in the transport equation for velocity,

$$\frac{\partial}{\partial t}\rho \boldsymbol{U} = -\boldsymbol{\nabla}.(\rho U \otimes U) - \nabla p + \mu \nabla.\nabla \boldsymbol{U} + \rho \boldsymbol{g} \qquad (3.11)$$

For a gas flow, the gravitational force can be neglected compared to other terms present in the equation, therefore the final governing equation for the gas phase velocity is,

$$\frac{\partial}{\partial t}\rho \boldsymbol{U} = -\boldsymbol{\nabla}.(\rho U \otimes U) + \mu \nabla.\nabla \boldsymbol{U} - \nabla p \qquad (3.12)$$

3.1.2 Species conservation equations

The transport equation for each species is obtained by considering the mass balance of respective species over an elemental volume as shown in Figure 3.2.

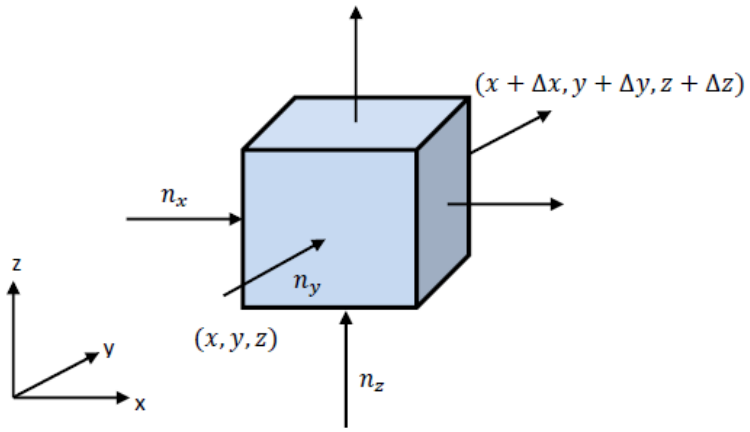

Figure 3.2 Differential volume element located in flow domain and mass fluxes across its faces

Mass balance equation can be written as [73],

$$\begin{Bmatrix} Rate\ of\ increase\ of \\ mass\ of\ species\ i \end{Bmatrix} = \begin{Bmatrix} Rate\ of \\ mass\ of \\ species\ i \\ into\ the \\ volume \\ element \end{Bmatrix} - \begin{Bmatrix} Rate\ of \\ mass\ of \\ species\ i \\ out\ of\ the \\ volume \\ element \end{Bmatrix} + \begin{Bmatrix} Rate\ of\ generation \\ of\ species\ i \end{Bmatrix}$$

The rate of mass of species *i* into the volume element is equal to,

$$n_i|_x \Delta y \Delta z + n_i|_y \Delta x \Delta z + n_i|_z \Delta x \Delta y$$

Where n_i is the mass flux vector of the i^{th} species.

Rate of mass of species *i* out of the control volume can be written as,

$$n_i|_{x+\Delta x} \Delta y \Delta z + n_i|_{y+\Delta y} \Delta x \Delta z + n_i|_{z+\Delta z} \Delta x \Delta y$$

Substituting these expressions into mass balance equation results in,

$$\Delta x \Delta y \Delta z \frac{\partial}{\partial t} \rho Y_i = \Delta y \Delta z (n_i|_x - n_i|_{x+\Delta x}) + \Delta x \Delta z \left(n_i|_y - n_i|_{y+\Delta y}\right) + \Delta x \Delta y (n_i|_z - n_i|_{z+\Delta z}) + r_i \Delta x \Delta y \Delta z \qquad (3.13)$$

Where r_i is the rate of generation of *i* through chemical reactions.

Dividing by $\Delta x\, \Delta y\, \Delta z$ and re arranging results in,

$$\frac{\partial}{\partial t} \rho Y_i = -\frac{n_i|_x - n_i|_{x+\Delta x}}{\Delta x} - \frac{n_i|_y - n_i|_{y+\Delta y}}{\Delta y} - \frac{n_i|_z - n_i|_{z+\Delta z}}{\Delta z} + r_i \qquad (3.14)$$

Taking the limit as Δx, Δy and Δz, go to zero results in the following partial differential equation,

$$\frac{\partial}{\partial t} \rho Y_i = \left(\frac{\partial n_i}{\partial x} + \frac{\partial n_i}{\partial y} + \frac{\partial n_i}{\partial z}\right) + r_i \qquad (3.15)$$

In vector notation, above equation can be written as,

$$\frac{\partial}{\partial t} \rho Y_i = -\nabla . n_i + r_i \qquad (3.16)$$

The mass flux vector n_i, consists of convective and diffusive mass transfer terms and is equal to [68],

$$n_i = j_i + \rho_i U \qquad (3.17)$$

Where ρ_i is the density of the i^{th} species and j_i is the diffusive flux of i^{th} species. j_i is given by Fick's law of molecular diffusion according to [73],

$$j_i = -\rho D_i \nabla Y_i \qquad (3.18)$$

Using above expression, n_i can be written as,

$$n_i = -\rho D_i \nabla Y_i + \rho Y_i U \quad (3.19)$$

Substituting in equation (3.16) and rearranging gives the governing transport equation for the species mole fraction Y_i

$$\frac{\partial}{\partial t}\rho Y_i + \nabla.(\rho Y_i U) - \nabla.(\rho D_i \nabla Y_i) = r_i \quad (3.20)$$

3.1.3 Drying models

Two major types of drying models were used in literature to obtain expressions for drying rates. They are first order kinetic models and equilibrium models [74].

3.1.3.1 First order kinetic model

This is the most common model used to describe drying in literature. The model expresses drying rate (r) by an Arrhenius type equation given by,

$$r = Aexp\left(\frac{-E}{RT_s}\right)\rho_{moisture} \quad (3.21)$$

where A (s^{-1}) is pre-exponential factor, E_a ($Jmol^{-1}$) is the activation energy, R ($Jmol^{-1}K^{-1}$) is the universal gas constant, T_s (K) and $\rho_{moisture}$ (kgm^{-3}) are solid phase temperature and density of water vapour at particle surface, respectively.

However, in the above global reaction scheme it is difficult to incorporate the effects of external factors such as air flow rate, air humidity, density, thermal conductivity, heat capacity and particle size on drying process. This limits the accuracy and scope of the final model because the model cannot be used to predict the impact of above mentioned properties.

3.1.3.2 Equilibrium model

Equilibrium models are used for predicting low temperature drying rates. These models are based on the assumption that water vapour is in equilibrium with liquid water. The rate is expressed as proportional to the driving force developed as a result of moisture deference at food particle surface and surrounding gas stream [17], [75]. The rate equation in equilibrium model is given by,

$$r = kA(\rho_{moisture} - \rho_{gas}) \quad (3.22)$$

where k (ms^{-1}) is the mass transfer coefficient and A [m^2m^{-3}] is the volumetric particle surface area. $\rho_{moisture}$ and ρ_{gas} [kgm^{-3}] are densities of water vapour at particle surface and in the gas phase respectively.

3.1.4 Mass balance equations

3.1.4.1 For Moisture fraction

The mass balance equation for moisture transport inside the copra is given by equation (3.23), which was derived by using equation (3.20)

$$\frac{\partial(\varphi\rho_w S_w)}{\partial t} + \nabla(U_w\rho_w) = \nabla(D_w\nabla\varphi\rho_w S_w) - I \qquad (3.23)$$

Where, S_w is the ratio of the amount of volume occupied by water to the available free space in the solid. With a similar definition for S_g which represents the gas phase,

$$S_w + S_g = 1 \qquad (3.24)$$

3.1.4.2 For vapour fraction

As the copra is heated, water evaporates, and eventually becomes water vapor. The gas inside the copra is a mixture of water vapor and air. ω_v and ω_a represent the mass fraction of vapor and mass fraction of air respectively.

$$\omega_v + \omega_a = 1 \qquad (3.25)$$

$$\frac{\partial(\varphi\rho_g S_g\omega_v)}{\partial t} + \nabla\left(U_g\rho_g\omega_v\right) = \nabla\left(D_v\nabla\varphi\rho_g S_g\omega_v\right) + I \qquad (3.26)$$

3.1.4.3 Rate of Evaporation

During the drying process, water evaporates and moves through the porous structure in copra. Equation (3.27) shows a non-equilibrium expression for evaporation of water [76].

$$I = k_{evp}\left(\rho_{v,eq} - \rho_v\right)S_g\varphi \qquad (3.27)$$

Where $\rho_{v,eq}$ is given by

$$\rho_{v,eq} = P_{sat}(-0.0267X^{1.656} + 0.0107e^{1.287X}X^{1.513}lnP_{sat}) \qquad (3.28)$$

3.1.4.4 Shrinkage and porosity

Since the solid volume is a conserved property, porosity at any time t (φ_t) can be determined by equating the initial volume of solid to solid volume at time *t*, [76]

$$(1 - \varphi_t)V_t = (1 - \varphi_0)V_0$$

Rearranging the equation with $^{V_t}/_{V_0} = J$,

$$\varphi_t = 1 - \frac{1-\varphi_0}{J} \qquad (3.29)$$

Where J is the jacobian due to moisture change. J is a direct measure of shrinkage and can be found experimentally as a function of moisture.

4. Numerical Solution

4.1 Introduction to OpenFOAM

OpenFOAM is an open source Computational Fluid Dynamics package which can be used to generate numerical solutions to mathematical models using finite volume method. Two main steps are involved in generating a numerical solution in OpenFOAM: setting up the case and setting up the solver. Case set up is the pre-processing stage in an OpenFOAM calculation. An OpenFOAM case is a collection of folders in which separate files are defined which contain the information on initial stage of the system and instructions on solving fluid dynamics equations. An example of a case file structure is illustrated in Figure 4.1.

The 0 folder consists of a set of files for each field for which solution is obtained (eg pressure and velocity). These files contain information on initial and boundary fields of these variables. Constant folder consists of a sub directory called polymesh where a blockMeshDict file is located. This file consists of information for mesh generation. Other files that are located in constant directory include transportProperties, physicalProperties and turbulanceProperties, which include information on values of physical constants (viscosity, thermal conductivity etc) and information on turbulence. Systems directory consist of files: ControlDict, fvSchemes and fvSolution. ControlDict file contains information on time control of the case, such as start time, end time, time step for numerical calculations and other information. fvSchemes consists of a list of discretization schemes for each variable. User can change discretization settings for the case by changing entries of this file. The fvSolution contains information about linear solvers that are used to solve discretized equations and tolerances for solved variables.

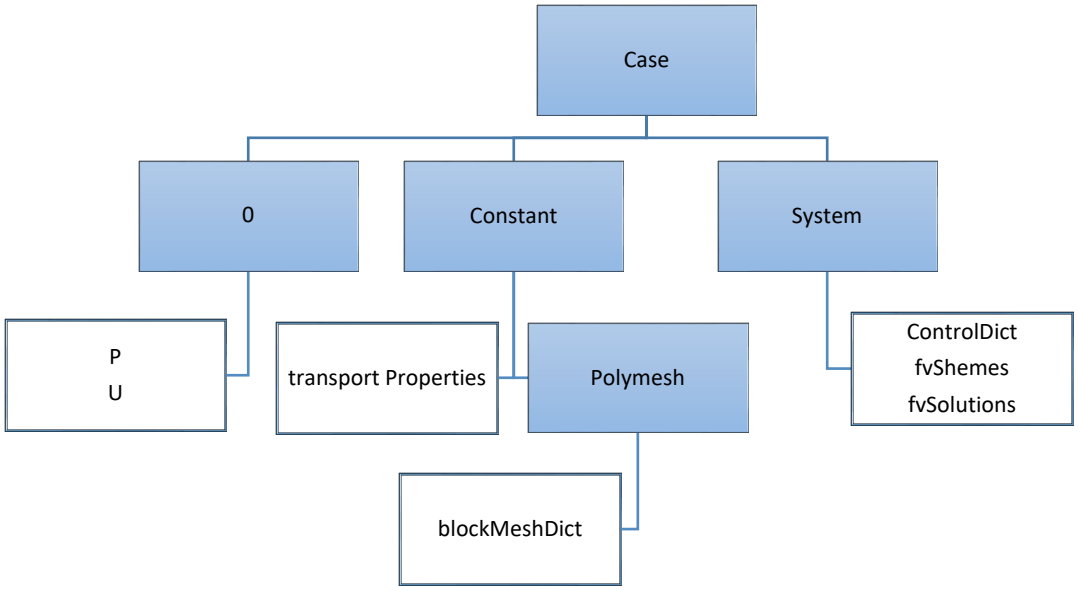

Figure 4.1 Structure of an OpenFOAM case

4.1.1 OpenFOAM solver

In OpenFOAM, a solver is a C++ library, which contains the code to numerically solve the relevant differential equations of the system of interest. Solvers can be classified as built in solvers and user compiled solvers. Built in solvers come with the original installation of OpenFOAM and can be used for solution of wide range of standard problems such as incompressible flow calculations, multiphase flows etc. When a built in solver cannot be applied to develop a solution to a particular problem, the user has the freedom to compile a new solver for the application. The OpenFOAM programming style allows user to declare and use mathematical quantities such as, scalars, vectors, tensors, their fields and differential equations. The differential equations are discretized using finite volume method. A brief introduction to finite volume discretization is presented in the following section.

4.2 Introduction to finite volume method

In numerical mathematics, partial differential equations are solved by first converting them to a corresponding set of algebraic equations. This is done by a method called discretization. There are a number of discretization techniques available such as

finite volume method, finite element method, finite difference method, spectral element method, boundary element method and high-resolution discretization schemes.

In the present study, the equations are discretized by finite volume method using the built in libraries of the CFD tool OpenFOAM. Finite volume discretization process can be divided into three main steps [77],

- Discretization of time
- Discretization of space
- Discretization of Equations

4.2.1 Discretization of time

Time is discretized by separating the time domain over which the solution is required into a set of time steps Δt, which may change during the simulation. During the solution procedure, time is marched from a prescribed initial condition.

4.2.2 Discretization of space

Discretization of space is achieved by sub dividing the solution geometry into a number of cells called control volumes. These cells should not overlap with one another and should fill the computational domain. The centroids of these cells determine the points of space at which the solution is required. A typical control volume and its associated properties are presented in Figure 4.2. The control volume is bounded by flat faces, represented by letter *f*. Cell faces belong to two main categories, internal faces and boundary faces. Internal faces are the faces between two control volumes and boundary faces coincide with boundaries of the solution domain. Each face of internal cells is shared with only one neighbour cell. Properties are usually defined at cell centroids, *P*. The face area vector, S_f is of magnitude equal to the area of the face and points outwards from the control volume perpendicular to the face [77].

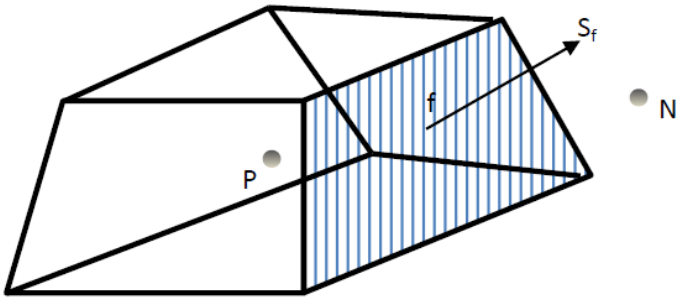

Figure 4.2 A typical control volume in finite volume method

4.2.3 Discretization of equations

The general form of the conservation equation for a scalar property can be written as,

$$\frac{\partial \emptyset}{\partial t} + div(\rho \emptyset u) - div(\tau grad \emptyset) = S_\emptyset \qquad (4.1)$$

The finite volume method requires that this equation should be satisfied in integral form over the control volume around the point at which the solution is sought [77]. This requires:

$$\int_t^{t+\Delta t} \left[\frac{\partial}{\partial t} \int \rho \emptyset dV + \int \nabla.(\rho U \emptyset) dV + \int \nabla.(\rho \Gamma \nabla \emptyset) dV \right] dt = \int_t^{t+\Delta t} (\int S_\emptyset dV) dt \qquad (4.2)$$

4.3.2.1 Spatial discretization

The first spatial term of equation (4.2) is discretized as,

$$\int \rho \emptyset dV = \rho \emptyset_p V_p \qquad (4.3)$$

The volume integrals of the above equation are converted into surface integrals over control volume surface using the following identities of vector calculus [78];

$$\int \nabla. A dV = \int A. dS \qquad (4.4)$$

$$\int \nabla. \emptyset dV = \int \emptyset dS \qquad (4.5)$$

This results in following relationship for convective and diffusive terms of the general conservation equation,

$$\int \nabla.(\rho U \emptyset) dV = \int (\rho U \emptyset). dS \qquad (4.6)$$

Since the control volume is bounded by a series of flat faces, the surface integral on the right hand side can be written as a sum of integrals over separate faces. Therefore

$$\int (\rho U \emptyset) dS = \sum_f \int (\rho U \emptyset). dS \qquad (4.7)$$

The face integral is evaluated using face value of $\emptyset$ and ρU and is given by

$$\int(\rho U\emptyset)dS = (\rho U)_f.S_f\emptyset_f \quad (4.8)$$

This provides the discretized form of the convective term as,

$$\int \nabla.(\rho U\emptyset)dV = \sum_f(\rho U)_f.S_f\emptyset_f \quad (4.9)$$

Using the above procedure, the laplacian term is discretized as,

$$\int \nabla.(\rho\Gamma\nabla\emptyset)dV = \int(\rho\Gamma\nabla\emptyset).dS$$
$$= \sum_f \int(\rho\Gamma\nabla\emptyset).dS$$
$$= \sum_f \rho\Gamma(\nabla\emptyset)_f.S_f$$

Therefore,

$$\int \nabla.(\rho\Gamma\nabla\emptyset)dV = \sum_f \rho\Gamma(\nabla\emptyset)_f.S_f \quad (4.10)$$

The discretized form of integral terms can be evaluated using face values and face centre values of neighbour cells. The entire set of discretized equations written over the solution domain represents a system of simultaneous linear equations. This linear set of equations is solved during each iteration of solution algorithm using numerical procedures for linear systems.

4.3 Development of CFD solver using OpenFOAM

Two new solvers, "2DcopradryingFoam" (for the determination of moisture diffusivity of first and second falling rate periods) and "3DcopradryingFoam" (for the determination of variable moisture diffusivity), were developed based on the equations presented in chapter 3. The equations are numerically solved using finite volume method and the required code was developed by using C++ language in OpenFOAM package. Input parameters and initial conditions for the CFD simulations were given in Table 4.1.

4.3.1 Boundary conditions

4.3.1.1 Two Dimensional model development

The two dimensional computational domain is shown in Figure 4.3. The computational domain is consisted with two parts. The lower part of the domain was considered as the copra sample and upper part of the domain was considered as the air layer near the top surface of the sample.

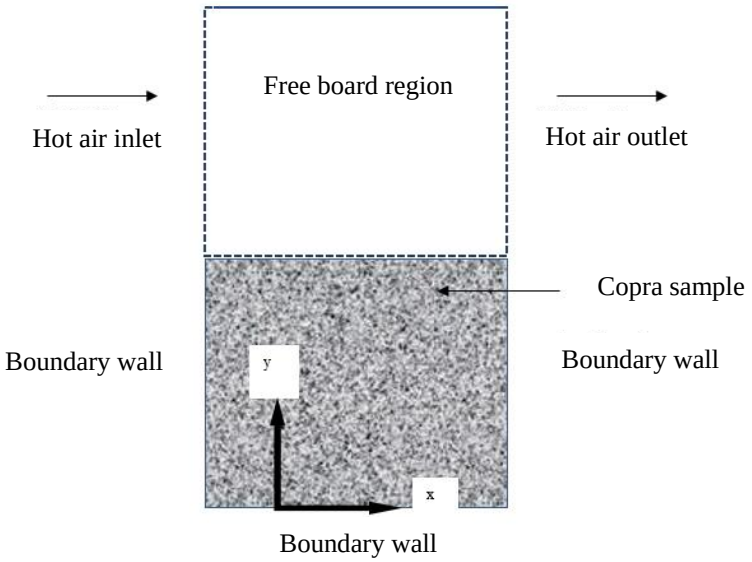

Figure 4.3 2D Computational domain

Wall boundary conditions

$U = 0$, $\frac{\partial P}{\partial x} = 0$, $\frac{\partial T_s}{\partial x} = 0$ and $\frac{\partial S_w}{\partial x} = 0$

Outlet boundary conditions

$\frac{\partial U}{\partial x} = 0$, $\frac{\partial P}{\partial x} = 0$, $\frac{\partial T_g}{\partial x} = 0$ and $\frac{\partial S_w}{\partial x} = 0$

4.3.1.2 Three dimensional model development

The three dimensional computational domain is shown in Figure 4.4.

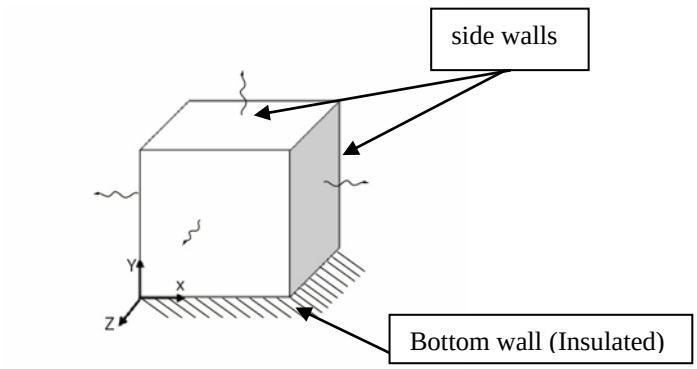

Figure 4.4 Schematic showing of boundary conditions

Side walls

$U = 0$, $\frac{\partial P}{\partial x} = 0$ and $\frac{\partial T_s}{\partial x} = 0$

Side walls are free surfaces available for forced convection and evaporation. Liquid water diffuses from the interior to the surface and leaves by convection as water vapor after evaporating at the surface. Therefore, liquid water flux ($n_{w/surf}$) at the surface is given by [79],

$$n_{w/surf} = k_m \varphi S_w (\rho_v - \rho_{amb}) \quad (4.11)$$

$$k_m = 0.5 \frac{h_t D_{bin} Le^{0.33}}{k_v} \quad (4.12)$$

$$D_{bin} = \frac{2.6\times10^{-5}(S_g\varphi)^{3-\varphi}}{\varphi} \quad (4.13)$$

$$Le = \frac{k_v}{\rho_a C_{p,a} D_{bin}} \quad (4.14)$$

$$h_t = 0.664 \left(\frac{k_a}{L}\right) Re^{0.5} Pr^{0.33} \quad (4.15)$$

$$Re = \frac{\rho U_a L}{\mu} \quad (4.16)$$

$$Pr = \frac{C_{p,a}\mu}{k_a} \quad (4.17)$$

Bottom wall

Since bottom wall was insulated for heat and mass transfer.

$U = 0$, $\frac{\partial P}{\partial x} = 0$, $\frac{\partial T_s}{\partial x} = 0$ and $\frac{\partial S_w}{\partial x} = 0$

Table 4.1 Input parameters for CFD simulation

Parameter	**Value**	**Units**
Atmospheric pressure (P)	101325	Pa
Characteristic length(L)	0.01	m
Density of water (ρ_w)	1000	kg/m^3
Density of vapor (ρ_v)	1.2	kg/m^3
Density of air (ρ_a)	1.2	kg/m^3
Evaporation rate constant (K_{evp})	0.01	1/s
Specific heat capacityair($C_{p,a}$)	1006	J/kgK
Thermal Conductivityvapor(k_v)	0.026	W/mK
Thermal Conductivity of air(k_a)	0.026	W/mK
Velocity of air(U_a)	0.1	m/s
Viscosity of water(μ)	$0.988x10^{-3}$	Pa s
Initial Conditions		
porosity(φ)	0.8	
Water fraction(S_w)	0.32	

5. Methodology

5.1 Materials

Coconut, which was seasoned for more than three weeks, was de-husked and split. Cubic samples of dimensions 0.01×0.01×0.01 m^3 (Figure 5.1) were cut from the kernel using a sharp knife. These samples were used in the drying experiments and shrinkage measurements.

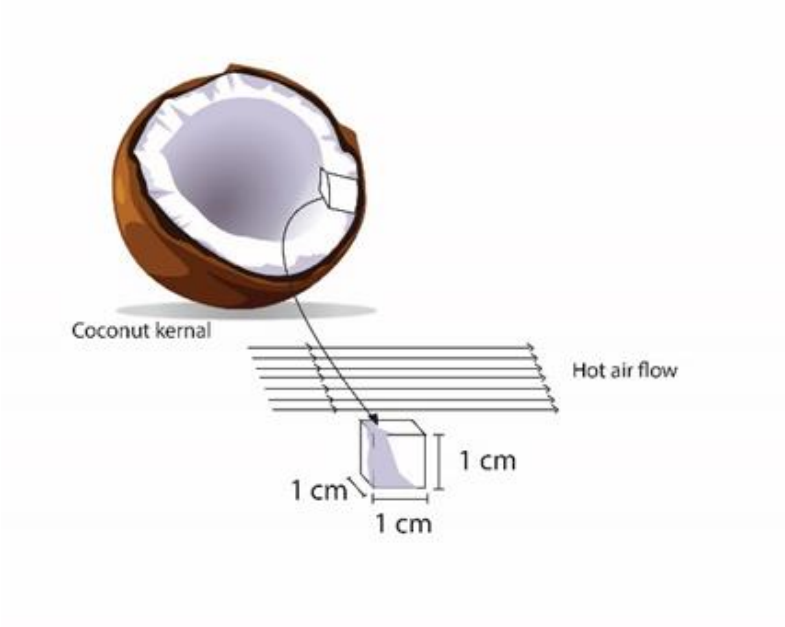

Figure 5.1 Copra sample

5.2 Experiment setup

5.2.1 Hot air dryer

An electric dryer is used to dry coconut pieces. The dryer consisted of a blower, an electrical heating element, temperature controlling switch and a drying chamber of 0.3×0.3×0.15 m^3 with a sample tray as shown in Figures 5.2 and 5.3

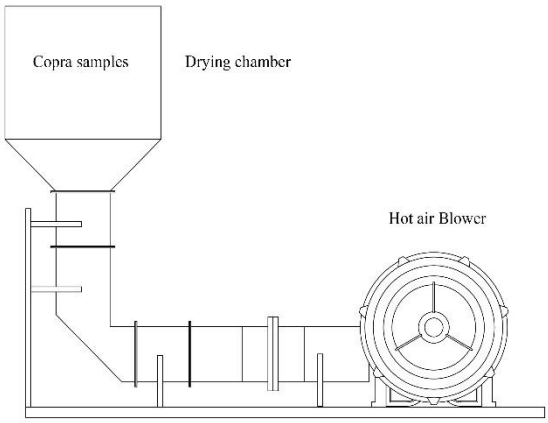

Figure 5.2 Sketch of the hot air dryer

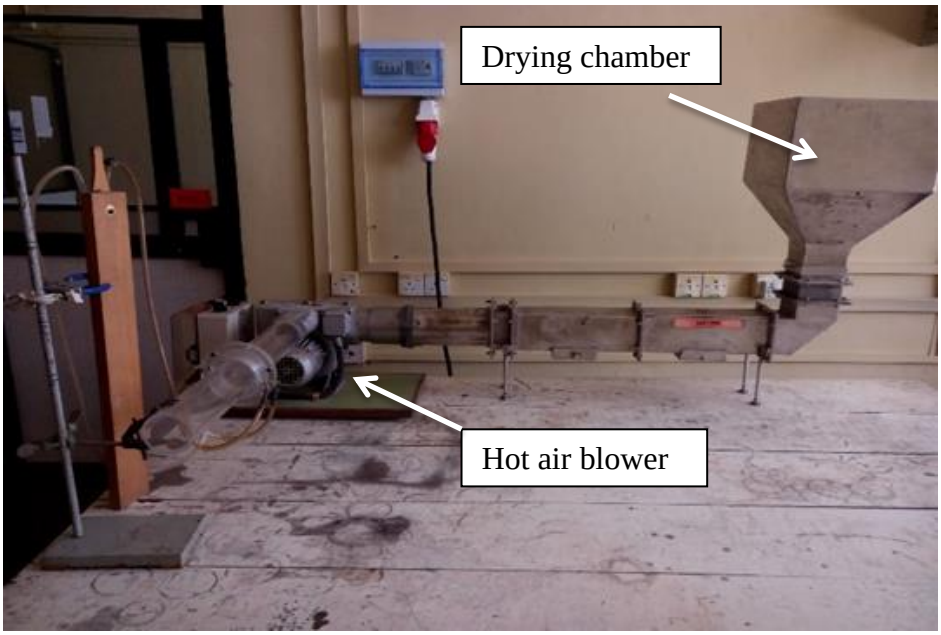

Figure 5.3 Photograph of hot air dryer

5.2.2 Experimental setup for volume measurement

An experimental setup consisting with Flask, Burette and Funnel was used to measure the volume of copra pieces by liquid displacement method as shown in Figure 5.4.

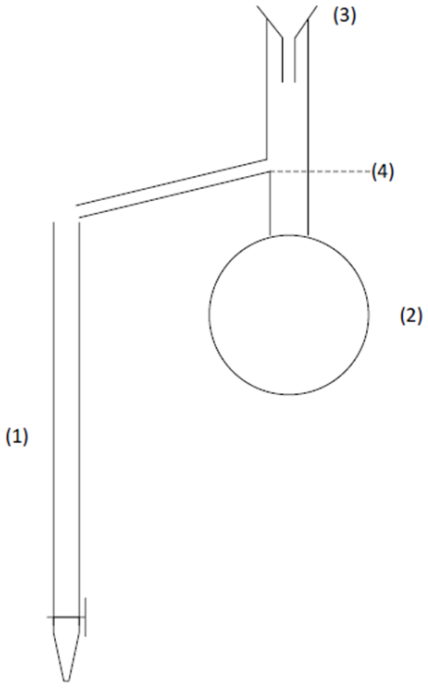

1. Burette (50ml)
2. Flask (250ml)
3. Funnel
4. Toluene level

Figure 5.4 Volume measuring setup

5.3 Determination of moisture diffusivity for first and second falling rate periods

5.3.1 Drying experiments to determine moisture diffusivity for first and second falling rate periods

Copra samples of dimensions 1×1×1 cm^3 were used with an average moisture content of 80 ± 0.8 % (w/w, dry basis). 60 samples were evenly placed as a single layer on the tray in the drying chamber. Relative humidity, hot air temperature, and hot air velocity were maintained at 40%, 55 °C and 0.1 ms^{-1}. The mass of each sample was separately measured using an electronic balance with an accuracy of ± 0.001 g in 2 hours intervals for 24 hours until the moisture content was reduced to 7 ± 0.5 %. (w/w, dry basis).

5.3.2 CFD Simulation with constant moisture diffusivity for 1st and 2nd falling rate periods

Governing differential equations (3.23-3.27) were numerically solved by finite volume method using open source CFD software OpenFOAM. Shrinkage was assumed to be negligible and therefore porosity was considered to be independent of moisture content. The error between experimental moisture content and simulated moisture content was calculated for assumed values of diffusion coefficient for 1st and 2nd falling rate periods. Simulation was continued by varying the assumed values of diffusion coefficient until the error was minimized.

5.4 Determination of shrinkage

Liquid displacement method [17], [49] was used to measure the initial volume ($V_{initial}$) and final volume (V_{final}) of the copra samples dried at 7 different hot air temperatures of 45, 50, 55, 60, 65, 70 and 75 °C. Toluene was used as the liquid in order to minimize the amount of liquid absorbed by the dried copra. For each measurement, three cubes of copra samples were randomly selected. Measurements were done in 15 minutes intervals during the first hour, 30 minutes intervals during the second and third hours and 60 minutes intervals for next 21 hours.

5.5 Development of moisture diffusivity model

5.5.1 Drying experiment for moisture diffusivity model

Similar to shrinkage measurements, drying experiments were also carried out for 7 different temperatures of 45, 50, 55, 60, 65, 70 and 75 °C. The constant air velocity of 0.1 ms^{-1}, the recommended velocity for industrial drying of copra was used for all the experiments [5].The relative humidity at drying chamber was maintained at 40%. The initial moisture content of the copra samples (0.01×0.01×0.01 m^3) were measured and the average was found as 80 ± 0.8 % (w/w, dry basis). Ten samples were randomly selected and evenly placed as a single layer on the tray in the drying chamber. Samples were weighed with the same time intervals as done for shrinkage measurements.

5.5.2 CFD Simulation for moisture diffusivity model

The open source CFD software OpenFOAM was used to develop a transient solver for the numerical solution of the proposed mathematical model. For slow drying processes, the gas pressure, p_g, within the material remains almost equal to atmospheric pressure and any flow arising due to gradients in gas pressure can be assumed small and neglected [79]. The net flux of liquid water was assumed to be given only by capillary diffusion and therefore, the convective term of equation (3.23) could be neglected.

The moisture content was predicted by using the numerical solution of Equation (3.23) for a given hot air temperature at a selected time by assuming values for diffusion coefficient [80]. The predicted moisture content was compared with the experimental data and simulation was carried out until the error was minimized. Since moisture diffusivity is a function of moisture content and drying temperature, the relationship among these parameters was developed using the computed diffusivity values. Mesh independence was investigated by increasing the cell number by 50% and 75% from initial value. Average moisture content at the same location in mesh at same time was compared under refined meshes. Since the deviation was found to be less than 1 % a three-dimensional mesh of 8000 cells were used for the CFD study.

6. Moisture Diffusivity for First and Second Falling Rate Periods

6.1 Drying characteristics of copra

The experimentally obtained drying curve is shown in Figure 6.1 and it clearly depicts two significant falling rate periods for copra drying process as most of other researchers found for similar food materials. And, this results suggests that copra has no constant rate period as same as for the other food materials such as such as tapioca, sugar beet root and avocado [25], [26], [27]. The drying curve also shows that the critical moisture content separating the first and second falling periods lies between moisture contents of 25 and 32 (%w/w, dry basis).

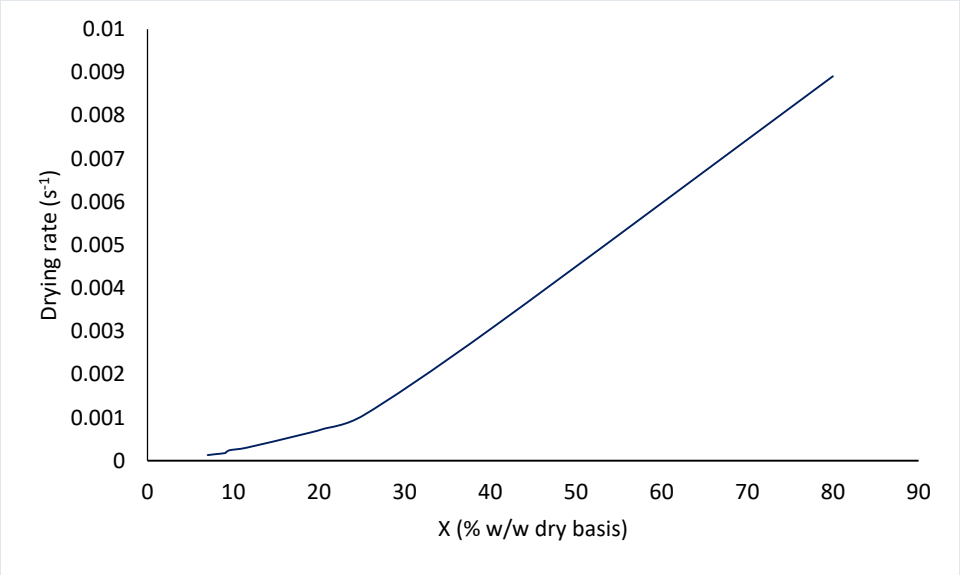

Figure 6.1 The graph of drying rate at 55 °C vs moisture content (% w/w dry basis)

6.2 Moisture diffusivity for 1st and 2nd falling rate periods

Two moisture diffusivity values were determined for two falling rate periods which were observed in experimental drying curve. The two initially assumed moisture diffusivity values were changed until the simulated drying curve was complying with the experimental drying curve. This process confirmed that the significant change in moisture diffusion was occurred at the moisture content of about 30% (w/w dry basis). Accordingly, the diffusion coefficient was found to have two values representing the first and the second falling rate periods at 55 °C as given below.

$$D_w = \begin{cases} 1.1 \times 10^{-8} & m^2 s^{-1} & M > 30\% \\ 1.9 \times 10^{-9} & m^2 s^{-1} & M < 30\% \end{cases} \quad (6.1)$$

Where, M - Moisture content.

Figure 6.2 shows that the experimental and simulated results of the variation of moisture content with respect to the drying time are in good agreement.

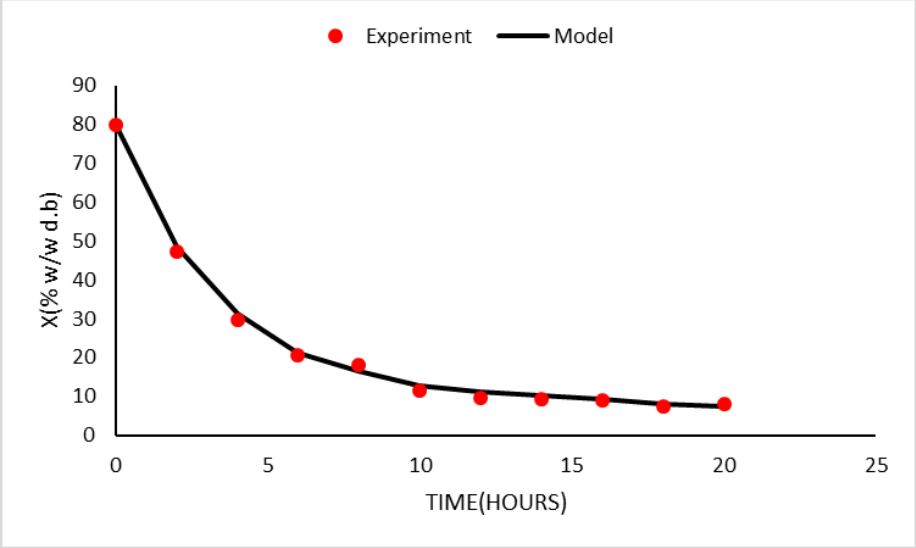

Figure 6.2 Experimental data vs Modeled data

The goodness of the fit of actual and predicted data were verified by values of coefficient of determination (R^2), root mean square error (RMSE) and reduced Chi square (χ^2) and the Chi-Square test [82], [83], [84] using Equation (6.2). The values of correlation coefficients of experimental and model data are given in Table 6.1.

Table 6.1 Correlation coefficients

R^2	RMSE	χ^2
0.9918	0.0134	0.0001

The hypotheses for the goodness of fit test are:

H0: There is no significant difference between the distribution of the sample and the modeled distribution

H1: There is a significant difference between the distribution of the sample and the modeled distribution.

The value of the Chi-square test was found to be 4.203. For the required significance level of 0.05 and the degrees of freedom of 10, with reference to Chi-square distribution table, the critical value of Chi-square was 18.307. Since the calculated value of Chi-square was less than this critical value the null hypothesis could not be rejected. Hence it can be concluded that both observed data and modeled data are from the same distribution.

$$\chi^2 = \sum_{i=1}^{N} \frac{(M_{exp,i} - M_{cal,i})^2}{M_{cal,i}} \qquad (6.2)$$

Where,

M_{exp} - Moisture content from experiment, M_{cal} - Moisture content from model and N - Number of observations.

6.3 Spatial distribution of moisture in the solid phase and the spatial distribution of vapor in the gas phase

Numerical results of Equation 3.23 and Equation 3.26 were used to obtain the spatial distribution of solid phase and gas phase moisture respectively. The spatial distributions of solid phase moisture content in different drying times are shown in Figures 6.3, 6.4 and 6.5. The spatial distribution of gas phase moisture content at steady state is shown in Figure 6.6. The spatial distribution results suggest that the equilibrium moisture content of 6% was achieved after 20 hours of drying at 55 °C and the moisture content was mostly varied in between 4 – 6 % (w/w, dry basis) within the copra.

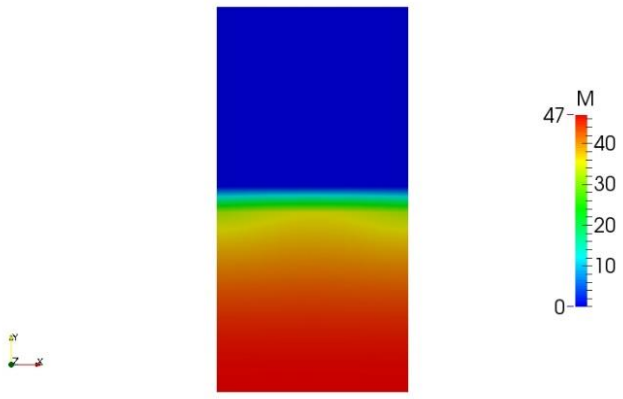

Figure 6.3 Spatial distribution of moisture content after 2 hours of drying time

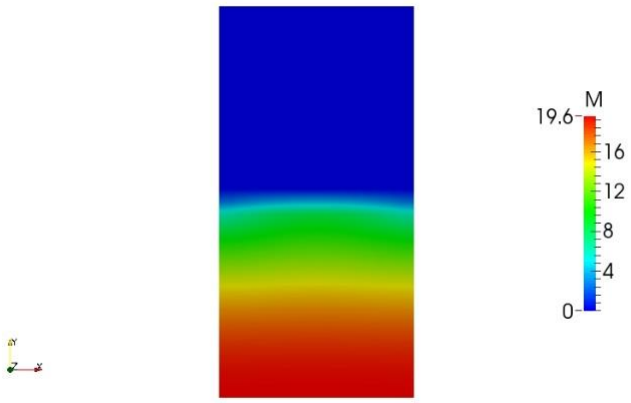

Figure 6.4 Spatial distribution of moisture content after 10 hours of drying time

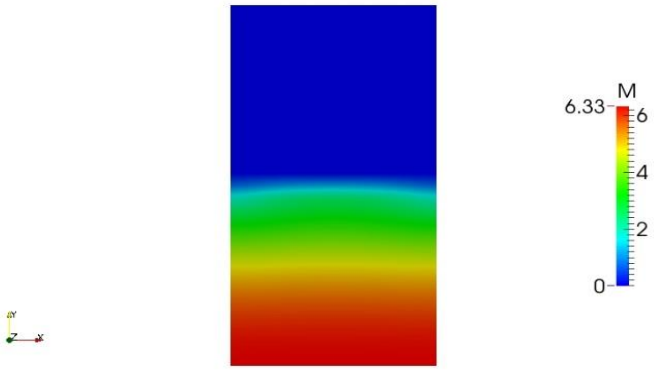

Figure 6.5 Spatial distribution of moisture content after 20 hours of drying time

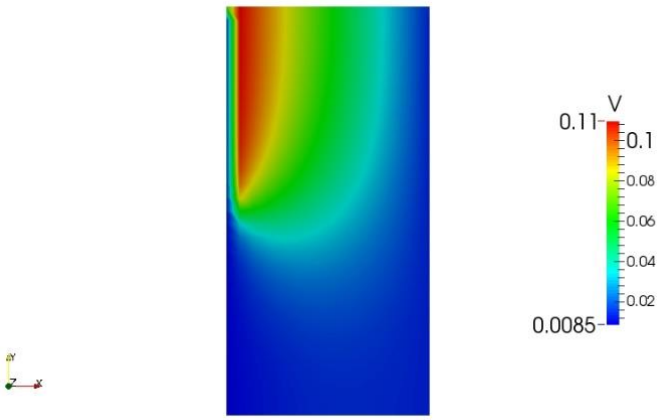

Figure 6.6 Spatial distribution of gas phase moisture content at steady state

7. Moisture Diffusivity Model

7.1 Shrinkage analysis

Shrinkage measurements were obtained for the hot air temperatures in the range of 45 – 75 °C. Figure 7.1 shows the variation of volume shrinkage (J) with respect to the moisture content (% w/w dry basis) for four different drying temperatures. The experimental results shown in Figure 7.1 indicate a linear variation which is independent of the hot air temperature. This observation is well in agreement with similar work carried out for potato chips, carrot slices and other similar food materials [38], [76], [85], [86], [87]. Therefore, a linear shrinkage model (Equation 7.1) is proposed for copra drying with the assumption that it is applicable to the range of temperatures tested in this study and the goodness of fit was verified by the values of coefficient of determination (R^2), root mean square error (RMSE) and reduced Chi square ($\chi 2$). The calculated values of R^2, RMSE and reduced $\chi 2$ for the seven different temperatures are shown in Table 7.1.

$$J = 0.0057X + 0.5331 \qquad (7.1)$$

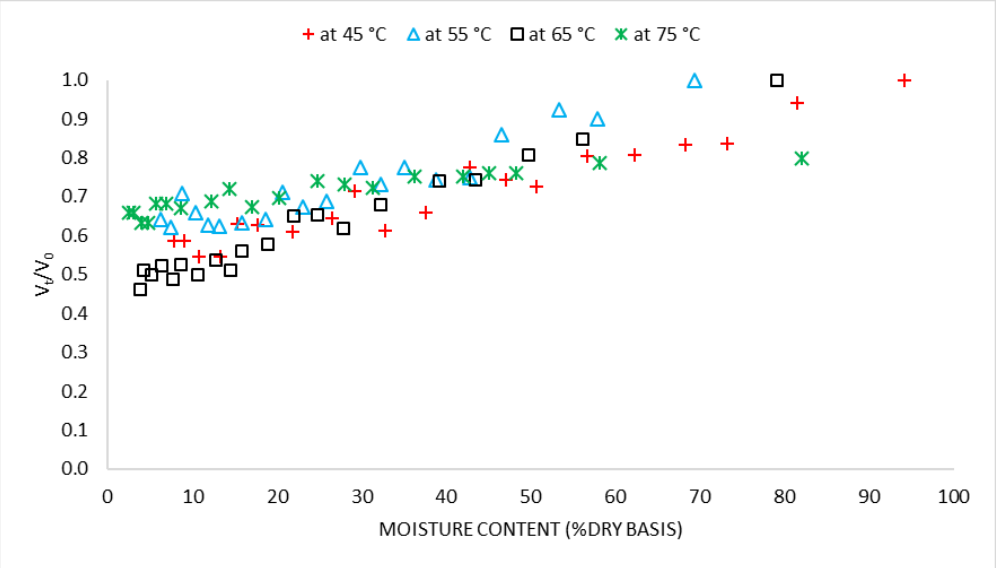

Figure 7.1 Plots of volume shrinkage vs moisture content

Table 7.1 Correlation coefficients of shrinkage model for different drying temperatures

Drying Temperature	R^2	RMSE	χ^2
45	0.7482	0.0651	0.0042
50	0.9054	0.0392	0.0015
55	0.8240	0.0529	0.0027
60	0.7282	0.0773	0.0059
65	0.9018	0.0583	0.0034
70	0.7973	0.0748	0.0055
75	0.9440	0.0509	0.0025

7.2 Diffusivity model

The simulated results of the predicted moisture diffusivity (*D*) against the moisture content (*X*) for the hot air temperatures examined in this study are shown in Figure 7.2. Based on these results, an exponential model (equation 7.2) with two exponential constants was proposed.

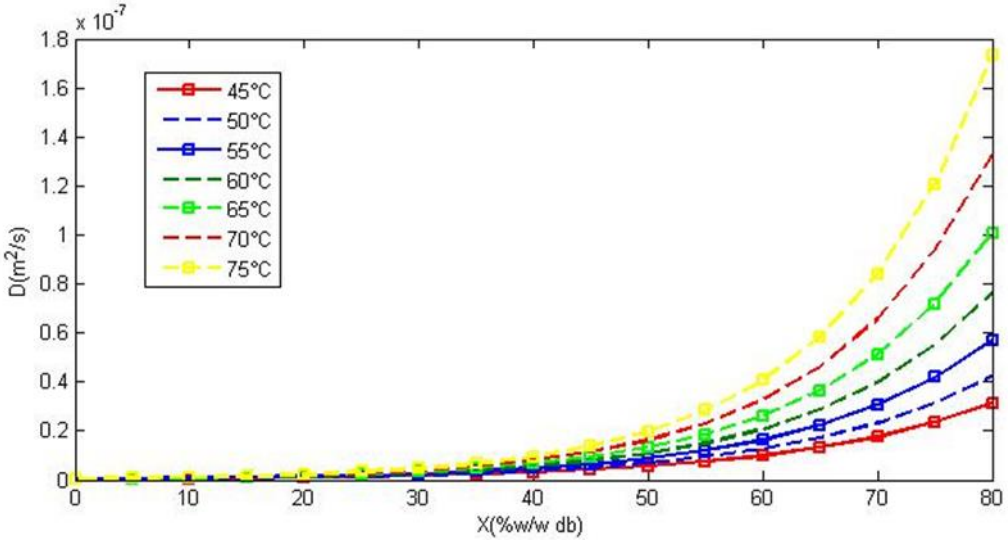

Figure 7.2 Plot of predicted moisture diffusivity vs moisture content

$$D(X,T) = (a)exp^{(b)X} \qquad (7.2)$$

Where *a* and *b* are constant for a given temperature, and found to be varied linearly with temperature

$a = a_1 + a_2T$ and $b = b_1 + b_2T$

The values of constants "a" and "b" for the seven different temperatures were obtained by curve fitting with the predicted moisture diffusivity data. Figures 7.3 and 7.4 indicate that both of the constants *a* and *b* linearly vary with the drying

temperature. The values of the models constant "a_1, a_2, b_1, b_2" of these two linear models are summarized in Table 7.2.

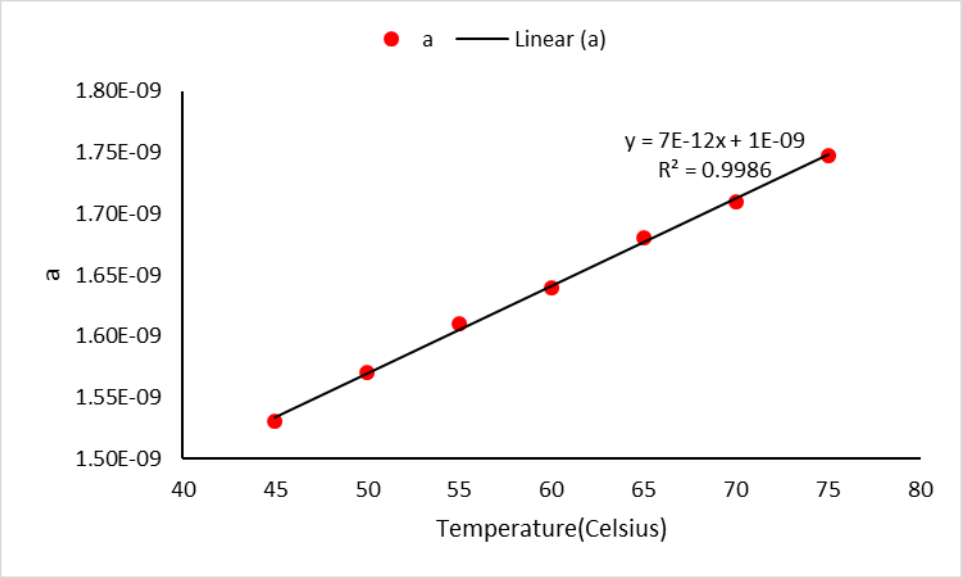

Figure 7.3 Plot of model constant" a" vs drying temperature

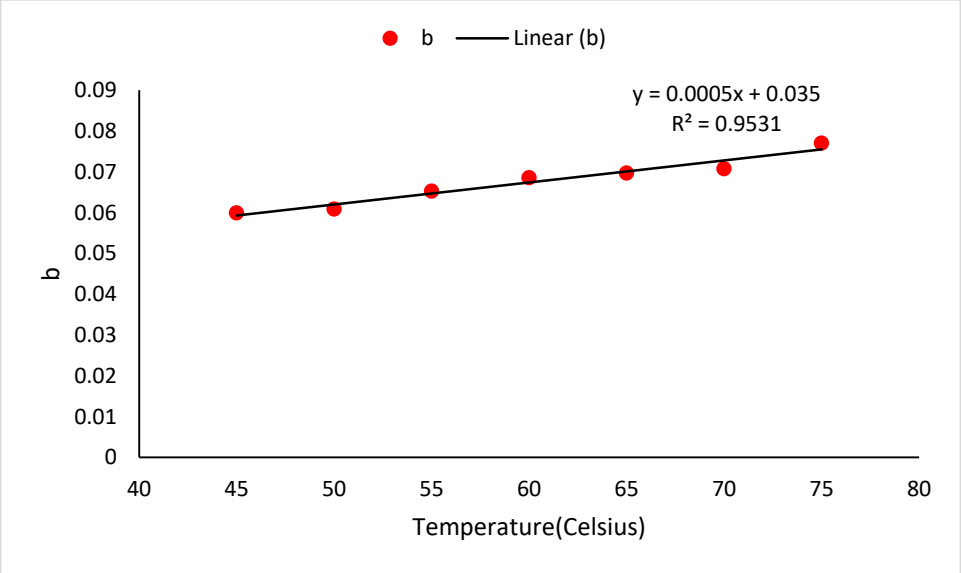

Figure 7.4 Plot of model constant" b" vs drying temperature

Table 7.2 Model constants for the proposed diffusivity model

a_1	a_2	b_1	b_2
10^{-9}	7×10^{-12}	0.035	0.0005

*These values are valid for copra drying using hot air in the temperature range 45°C to 75°C

7.3 CFD simulation using variable diffusion coefficient

Using the proposed shrinkage model (Equation 7.1) and the diffusion model (Equation 7.2), the numerical model (Equations 3.23 to 3.29) was solved and the spatial distribution of moisture in the copra sample was obtained by CFD simulation using OpenFOAM software. The variation of average moisture content vs time for a given temperature was predicted and validated using the experimental values. Figure 7.5 shows the predicted and actual drying curves for temperatures 45, 55, 65 and 75 ^{o}C (Only four temperatures are presented for clarity). Figure 7.5 indicates a good match between predicted and experimental data and the goodness of fit were verified by the values of coefficient of determination (R^2), root mean square error (RMSE) and reduced Chi square ($\chi 2$). For a good fit RMSE value and reduced $\chi 2$ value should be closed to zero and R^2 value should be closed to 1 [88], [89], [90], [91]. The calculated values of R^2, RMSE and reduced $\chi 2$ for the seven different temperatures shown in Table 7.3 suggest a good correlation between the experimental and computed data.

Table 7.3 Statistical evaluation of experimental and modeled data for different drying temperatures

Drying Temperature	R^2	RMSE	χ^2
45	0.9956	0.0160	0.0003
50	0.9979	0.0115	0.0001
55	0.9945	0.0173	0.0003
60	0.9947	0.0187	0.0004
65	0.9922	0.0231	0.0005
70	0.9945	0.0201	0.0004
75	0.9927	0.0233	0.0005

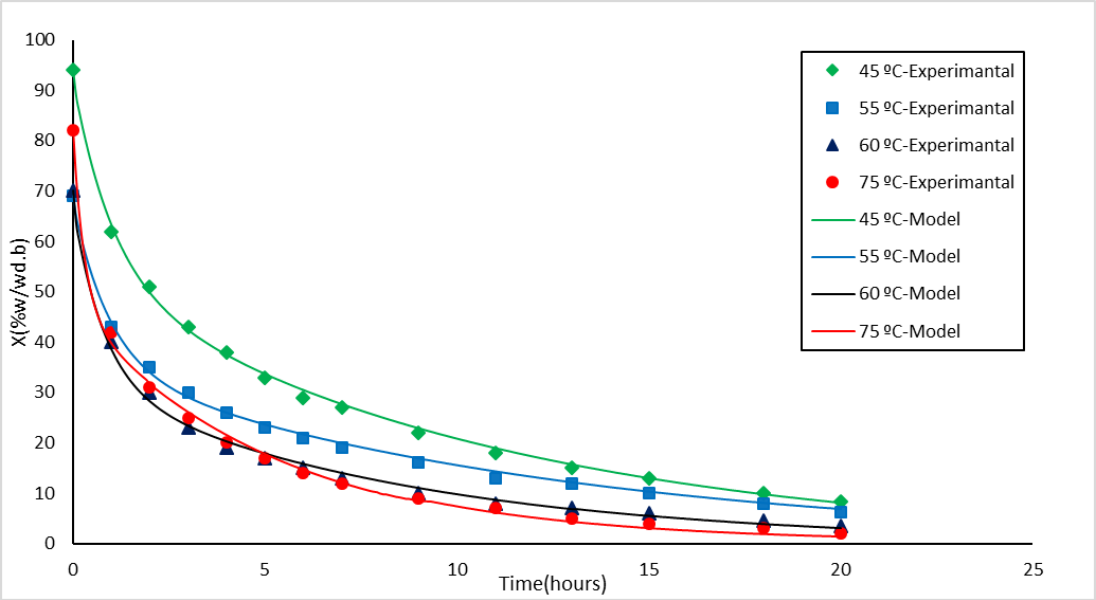

Figure 7.5 Actual and predicted moisture content (% w/w d.b) vs drying time

The numerical results of spatial distribution of moisture inside the copra after 20 hours of drying time are shown in Figures 7.6 and 7.7. Table 7.4 summarizes these results. The desired moisture content of copra is about 7 % (w/w, d.b) [1], [3], [4] and the results given in Figures 7.6 and 7.7 suggest that equilibrium moisture content could be achieved within 20 hours of drying for hot air temperatures equal or above 60 ºC. The predicted and actual data given in Table 7.4 confirm this observation. Therefore the optimum temperature for copra drying can be identified as 60 ºC which is in agreement with the previously reported research on copra drying [7], [8].

Table 7.4 Summary of Simulated results for drying after 20 hours

Drying Temperature (°C)	**Spatial moisture content (w/w % d.b.)**		**Average moisture content (w/w % d.b.)**	
	Maximum	Minimum	Estimated	Experimental
45	8.6	7.3	8.1	9.1±0.3
50	7.2	6.1	6.8	7.5±0.2
55	7.0	5.9	6.6	7.0±0.3
60	4.4	3.2	3.8	4.5±0.2
65	4.2	3.0	3.7	4.2±0.3
70	4.0	2.8	3.6	4.2±0.3
75	2.7	1.6	2.3	3.0±0.2

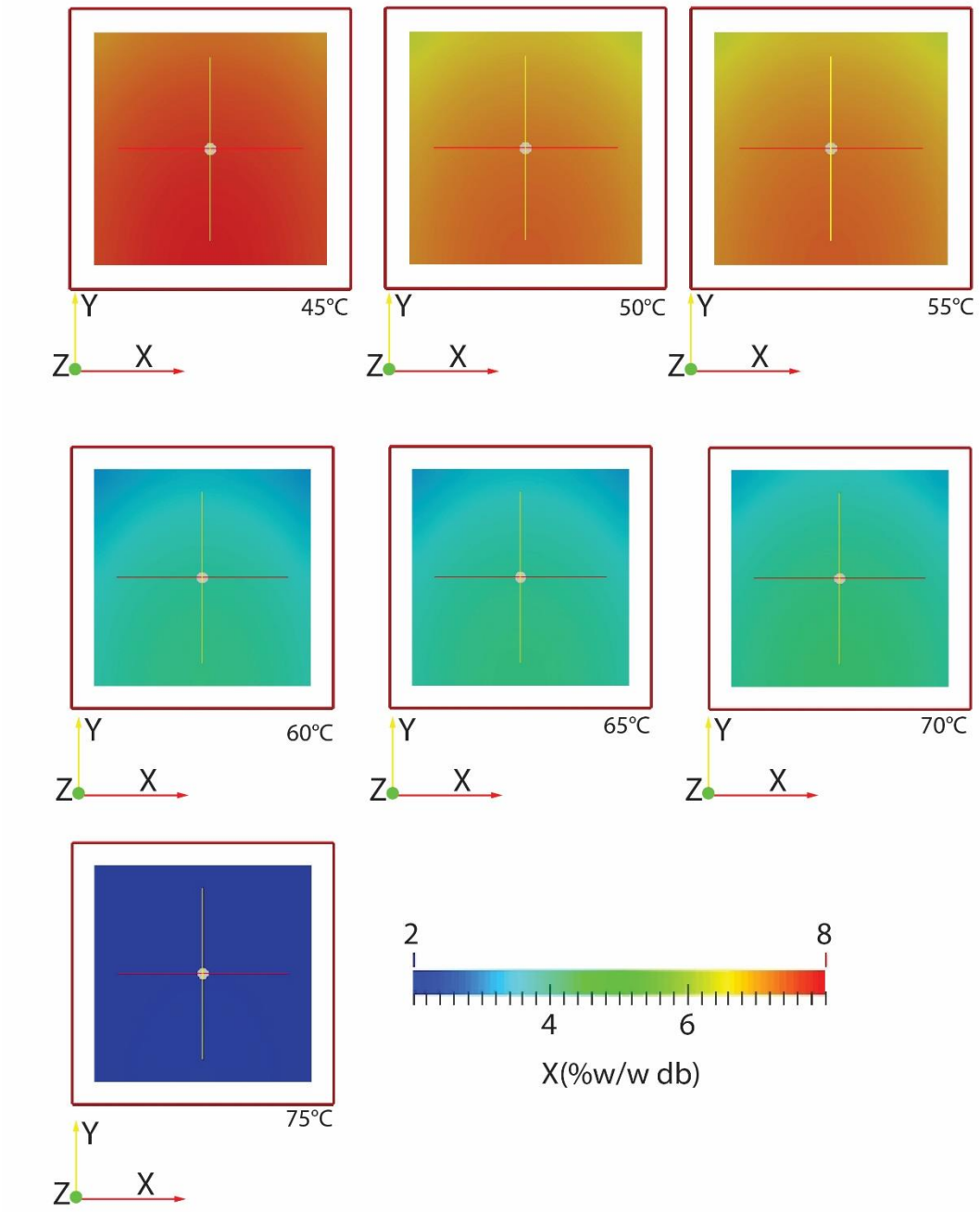

Figure 7.6 2-D Spatial distribution of moisture content at the cross section through the center of copra cube of 1cm3after 20 hours of drying

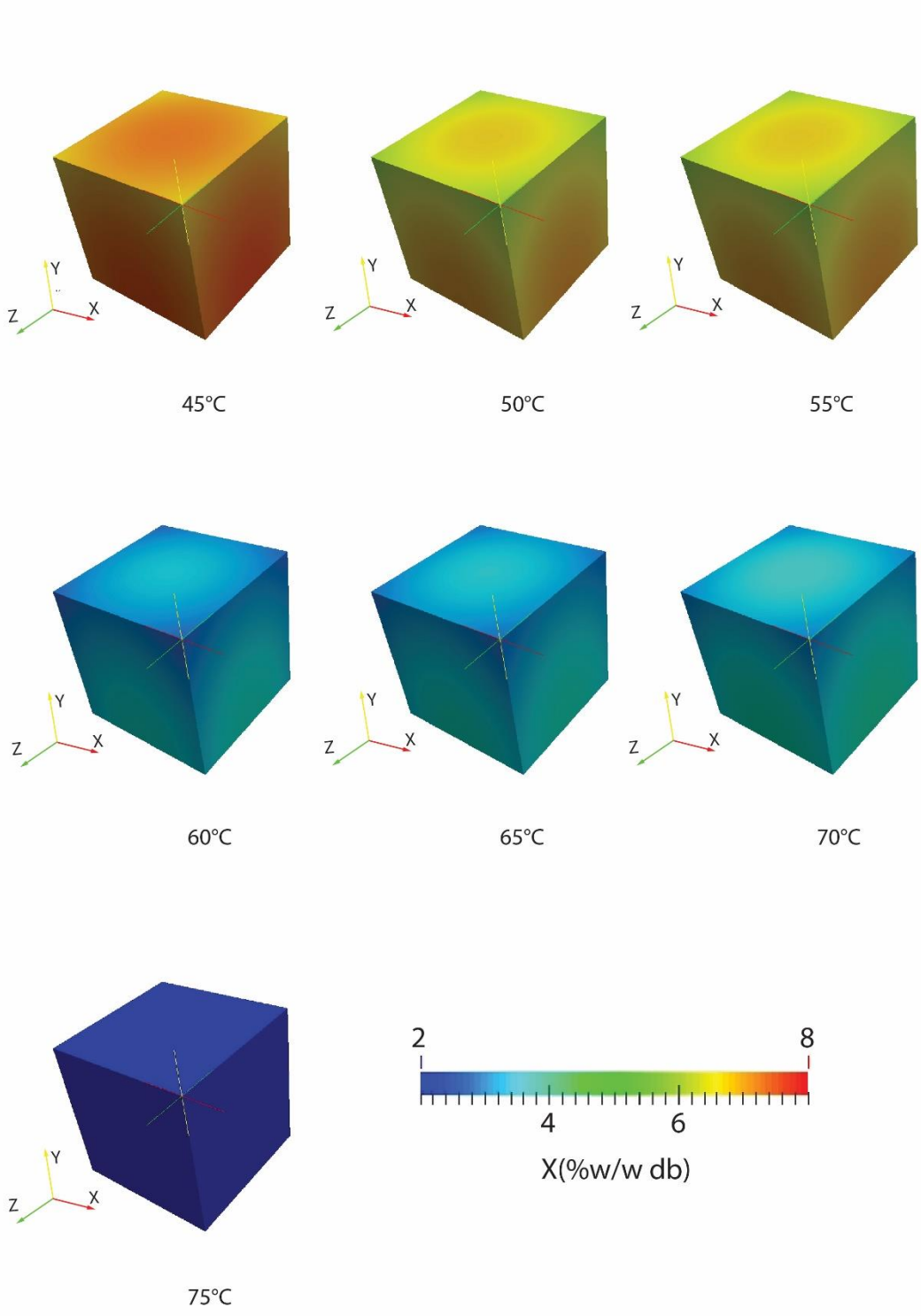

Figure 7.7 Outer surface spatial distribution of moisture content of the 1cm3copra

8. Conclusion and Future Works

8.1 Conclusions

8.1.1 Determination of moisture diffusivity for first and second falling rate periods

Two significantly different sub-drying periods were observed in the hot air drying of copra corresponding to first and second falling rate periods. The effective moisture diffusivity for the first and second falling rate periods at 55 °C were estimated using numerical model as 1.10×10^{-8} and 1.99×10^{-9} m^2s^{-1} respectively. Further the model suggested that the critical moisture content which separates the sub-drying periods was found to be 30% (w/w, dry basis). The spatial distribution results indicated that the moisture content majorly varied in between 4 – 6 % (w/w, dry basis) within the copra at 55 °C after achieving the equilibrium moisture content of 6% in 20 hours.

8.1.2 Development of the moisture diffusivity model

An exponential function $D(X,T) = (a)exp^{(b)X}$, was proposed to predict the diffusivity of moisture inside copra. The model constants, a and b, were found to linearly vary with temperature as $a = a_1 + a_2T$ and $b = b_1 + b_2T$. For the range of hot air temperatures from 45 – 75 °C, the values of a_1, a_2, b_1 and b_2 were found to be 10^{-9}, 7×10^{-12}, 0.04 and 0.0005 respectively. Further the moisture content was also found to have a linear relationship with the shrinkage, $J = 0.0057X + 0.5331$. A numerical model was developed using these relationships and the drying curves were predicted for copra drying. The actual and the predicted data were found to have a good correlation with the coefficient of determination (R^2) close to 1, Root mean square error (RMSE) and reduced chi-square (χ^2) close to zero. The results of the spatial distribution of moisture inside copra after 20 hours of drying suggested the optimum drying temperature of 60 °C which complies with the previous works on copra drying.

8.2 Future recommendations

The presented mathematical model can be used as a numerical tool to optimize the hot air copra drying process. The analysis on copra by the methods of mathematical modelling and simulation can be extended to evaluate the moisture diffusivity of similar porous structures like food items.

References

[1]. M. Meedenya and R. Coorey, "Quality Assessment of Commercially Available Coconut Oils in Sri Lanka Using Refractometry," Proc. Tech. Sess., vol. 28, pp. 37–44, 2012.

[2]. E. C. Canapi, Y. T. V Agustin, E. A. Moro, E. J. Pedrosa, and M. L. J. Bendano, Coconut Oil. 2015.

[3]. M. Mohanraj and P. Chandrasekar, "Drying of copra in a forced convection solar drier," Biosyst. Eng., 2008.

[4]. M. C. P. Rodrigo, B. L. Arnarasiriwardene, and U. Samarajeewa, "some observations on copra drying in sri lanka," 1996.

[5]. R. C. Guarte, W. Mühlbauer, and M. Kellert, "Drying characteristics of copra and quality of copra and coconut oil," Postharvest Biol. Technol., 1996.

[6]. T. Thanaraj, N. D. A. Dharmasena, and U. Samarajeewa, "Comparison of quality and yield of copra processed in CRI improved kiln drying and sun drying," J. Food Eng., vol. 78, no. 4, pp. 1446–1451, Feb. 2007.

[7]. M. Mohanraj and P. Chandrasekar, "Comparison of drying characteristics and quality of copra obtained in a forced convection solar drier and sun drying," J. Sci. Ind. Res. (India)., vol. 67, no. 5, pp. 381–385, 2008.

[8]. T. Thanaraj, D. Dharmasena, and U. Samarajeewa, "Development of a Rotary Solar Hybrid Dryer for Small Scale Copra Processing," Trop. Agric. Res, 2004.

[9]. M. A. Satter, "optimization of copra drying factors by taguchi method," pp. 23–27, 2001.

[10]. I. Zlatanović, M. Komatina, and D. Antonijević, "Low-temperature convective drying of apple cubes," Appl. Therm. Eng., 2013.

[11]. D. Mitrea and A. Datta, “Porous Media Based Model for Deep Frying Potato Chips in a Vacuum,” 2010.

[12]. D. A. Tzempelikos, D. Mitrakos, A. P. Vouros, A. V. Bardakas, A. E. Filios, and D. P. Margaris, “Numerical modeling of heat and mass transfer during convective drying of cylindrical quince slices,” J. Food Eng., 2015.

[13]. V. T. Karathanos, G. Villalobos, and G. D. Saravacos, “Compar- ison of two methods of estimation of the effective moisture diffusivity from drying data,” J. Food Eng., 1990.

[14]. S. S. Kim and S. R. Bhowmik, “Effective moisture diffusivity of plain yogurt undergoing microwave vacuum drying,” J. Food Eng., 1995.

[15]. R. B. Keey, “Drying principles and practices.,” Oxford, New York Pergamon Press., 1972.

[16]. G. P. Sharma and S. Prasad, “Effective moisture diffusivity of garlic cloves undergoing microwave-convective drying,” J. Food Eng., 2004.

[17]. R. E. Treybal, Mass transfer operations, 3rd ed. Tokyo: McGraw- Hill, Kogakusha Ltd.., 1980.

[18]. An introduction about coconut industry, Copra and coconut oil industry, by Marketing development and research division, Coconut development authority, Sri Lanka, 1997.

[19]. Fereidoon Shahidi, Bailey’s Industrial Oil and Fat Products, 6th ed. 2005.

[20]. P. Malabrigo, “Drying, storage, and preparation of copra for extraction of oil,” J. Am. Oil Chem. Soc., 1977.

[21]. Gamage, T.V. Samarajeewa, and S. N. U. Arseculeratne, “Aflatoxin contamination and free fatty acid content of coconut oil from small-scale mills,” in. Natn. Sci. Coun. Sri Lanka, 1983.

[22]. M. Varnakulasingam, “Quality Standards for Coconut Products.,” in Asian Coconut Community. CO- COPEP Bi-Annual Meeting, Quezon., 1974.

[23]. Satter, M. A,“Design and development of a portable copra dryer”, Proceedings of the International Conference on Mechanical Engineering, Dhaka, Bangladesh,2003.

[24]. Satter, M. A, “Optimization of Copra Drying Factors by Taguchi Method”, 4th International Conference on Mechanical Engineering, Dhaka, Bangladesh/pp. III 23-27,2001.

[25]. Geankoplis, C.J. Transport Processes and Unit Operations, 3rd ed.; Prentice Hall: Englewood Cliffs, NJ, 1993.

[26]. Saravacos, G.D.; Charm, S.E. “A Study of the Mechanism of Fruit and Vegetable Dehydration”, Food Technol. 1962

[27]. Rizvi, S.S.H. “Thermodynamic Properties of Foods in Dehydration”, In Engineering Properties of Foods, 3rd ed.; Rao, M.A.; Rizvi, S.S.H.; Datta, A.K.; Eds.; Marcel Dekker, Inc.: New York,2005.

[28]. Vaccarezza, L.M.; Lombardi, J.L.; Chirife, J. “Kinetics of Moisture Movement during Air Drying of Sugar Beet Root”, J. Food Technol. 1974.

[29]. Alzamora, S.M.; Chirife, J. “Some Factors Controlling the Kinetics of Moisture Movement during Avocado Dehydration”, J. Food Sci. 1980.

[30]. Karel, M.; Lund, D.B. Physical Principles of Food Preservation, 2nd ed.; Marcel Dekker, Inc.New York, 2003.

[31]. Chirife, J. “Fundamentals of the Drying Mechanism during Air Dehydration of Foods”, In Advances in Drying; Mujumdar, A.S.; Ed.; Hemisphere Publishing Corp.: Washington, DC, 1983.

[32]. Chirife, J. Diffusional Process in the Drying of Tapioca Root. J. Food Sci. 1971

[33]. Jason, A.C. “A Study of Evaporation and Diffusion Processes in the Drying of Fish Muscle”, In Fundamental Aspects of Dehydration of Foodstuffs; Soc. Chem. Ind.: London and MacMillan Co.: New York, 1958.

[34]. W.A.M. McMinn and T.R.A. Magee, “Principles, Methods and Applications of the Convective Drying of Foodstuffs,” Food Bioprod. Process., 1999.

[35]. A.S. Mujumdar, Handbook of Industrial Drying. Taylor and Francis Group, LLC, 2006.

[36]. S. Azzouz, A. Guizani, W. Jomaa, and A. Belghith, “Moisture diffusivity and drying kinetic equation of convective drying of grapes,” J. Food Eng., 2002.

[37]. E. Akpinar, A. Midilli, and Y. Bicer, “Single layer drying behaviour of potato slices in a convective cyclone dryer and mathematical modeling,” Energy Convers. Manag., 2003.

[38]. L. Hassini, S. Azzouz, R. Peczalski, and A. Belghith, “Estimation of potato moisture diffusivity from convective drying kinetics with correction for shrinkage,” J. Food Eng., 2007.

[39]. I. Doymaz, “Convective air drying characteristics of thin layer carrots,” J. Food Eng., 2004.

[40]. Velic´, D.Planinic, M.Tomas, and B. S., “Influence of airflow velocity on kinetics of convection apple drying,” J. Food Eng. , 2004.

[41]. K. Sacilik and A. K. Elicin, “The thin layer drying characteristics of organic apple slices,” J. Food Eng., vol. 73, no. 3, pp. 281–289, 2006.

[42]. I. Zlatanović, M. Komatina, and D. Antonijević, “Low-temperature convective drying of apple cubes,” Appl. Therm. Eng., vol. 53, no. 1, pp. 114–123, 2013.

[43]. N. Wang and J. G. Brennan, “A mathematical model of simultaneous heat and moisture transfer during drying of potato,” Journal of Food Engineering. 1995.

[44]. W. Aregawi, T. Defraeye, S. Saneinejad, P. Vontobel, E. Lehmann, J. Carmeliet, P. Verboven, D. Derome, and B. Nicolai, “Understanding forced convective drying of apple tissue: Combining neutron radiography and numerical modelling,” Innov. Food Sci. Emerg. Technol., vol. 24, pp. 97–105, 2014.

[45]. A. K. Datta, “Porous media approaches to studying simultaneous heat and mass transfer in food processes. I: Problem formulations,” J. Food Eng., vol. 80, no. 1, pp. 80–95, 2007.

[46]. J. Zhanga and A. K. Dattaa*, “Some Considerations in Modeling of Moisture Transport in Heating of Hygroscopic Materials,” Dry. Technol., 2007.

[47]. T. Defraeye, “Advanced computational modelling for drying processes – A review,” Appl. Energy, vol. 131, pp. 323–344, 2014.

[48]. E. Barati and J. A. Esfahani, “A new solution approach for simultaneous heat and mass transfer during convective drying of mango,” J. Food Eng., vol. 102, no. 4, pp. 302–309, 2011.

[49]. M. Ateeque, R. K. Mishra, V. P. Chandramohan, and P. Talukdar, “Numerical modeling of convective drying of food with spatially dependent transfer coefficient in a turbulent flow field,” Int. J. Therm. Sci., 2014.

[50]. Jost, W. Fundamental Laws of Diffusion. In Diffusion in Solids, Liquids, Gases; Hutchinson, E.;Ed; Academic Press Inc.: New York, 1952.

[51]. Lewis, W.K. The Rate of Drying of Solid Materials. Ind. Eng. Chem. 1921

[52]. Sherwood, T.K. The Drying of Solids—I. Ind. Eng. Chem. 1929

[53]. Sherwood, T.K. The Drying of Solids—II. Ind. Eng. Chem. 1929

[54]. Ceaglske, N.H.; Hougen, O.A. The Drying of Granular Solids. Trans. Am. Inst. Chem. Eng.1937

[55]. Hougen, O.A.; McCauley, H.J.; Marshall, W.R., Jr. Limitations of Diffusion Equations. Trans.Am. Inst. Chem. Eng. 1940

[56]. Hawlader, M.N.A.; Uddin, M.S.; Ho, J.C.; Teng, A.B.W. “Drying Characteristics of Tomatoes”, J.Food Eng. 1991

[57]. Ede, A.J.; Hales, K.C. “The Physics of Drying in Heated Air, with Special Reference to Fruit and Vegetables”, G. Brit. Dept. Sci. Ind. Res., Food Invest. Spec. Rept. 53, 1948.

[58]. Saravacos, G.D.; Maroulis, Z.B. “Transport Properties of Foods”, Marcel Dekker: New York,2001.

[59]. Van Arsdel, W.B. “Approximate Diffusion Calculations for the Falling-rate Phase of Drying”,Trans. Am. Inst. Chem. Eng. 1947

[60]. Sablani, S.; Rahman, S.; Al-Habsi, N. “Moisture Diffusivity in Foods An Overview”, In Drying Technology in Agriculture and Food Sciences; Mujumdar, A.S.; Ed.; Science Publishers, Inc.: Enfield, NH, 2000.

[61]. Luyben, K.A.M.; Olieman, J.J.; Bruin, S. “Concentration Dependent Diffusion Coefficients Derived from Experimental Drying Curves”, In Drying ’80; Mujumdar, A.S.; Ed.; Hemisphere Publishing Corp.: New York, 1980.

[62]. Singh, R.K.; Lund, D.B.; Buelow, F.H. “An Experimental Technique Using Regular Regime Theory to Determine Moisture Diffusivity”, In Engineering and Food; McKenna, B.M.; Ed.;Elsevier Applied Science Publ.: London, 1984.

[63]. Crank, J. The Mathematics of Diffusion, 2nd ed.; Oxford University Press: London, 1975.

[64]. Fish, B.P. “Diffusion and Thermodynamics of Water in Potato Starch Gel”, In Fundamental Aspects of Dehydration of Foodstuffs; Soc. Chem. Ind., London and MacMillan Co.: New York,1958.

[65]. Gekas, V.; Lamberg, I. “Determination of Diffusion Coefficients in Volume-changing Systems Application in the Case of Potato Drying”, J. Food Eng. 1991.

[66]. Khraisheh, M.A.M.; Cooper T.J.R.; Magee, T.R.A. “Shrinkage Characteristics of Potatos Dehydrated under Combined Microwave and Convective Air Conditions”, Drying Technol. 1997.

[67]. Madamba, P.S.; Driscoll, R.H.; Buckle, K.A. “Shrinkage, Density, and Porosity of Garlic during Drying”, J. Food Eng. 1994.

[68]. Mulet, A.; Berna, A.; Borras, M.; Pinaga, F. “Effect of Air Flow Rate on Carrot Drying”, Drying Technol. 1987.

[69]. Simal S.; Rossello C.; Berna, A.; Mulet, A. “Drying of Shrinking Cylinder-shaped Bodies”, J.Food Eng. 1998.

[70]. T. M. Afzal and T. Abe, “Diffusion in potato during far infrared radiation drying,” J. Food Eng., 1998.

[71]. Baik.O. D. and M. Marcotte, “Modeling the moisture diffusivity in a baking cake,” J. Food Eng., 2003.

[72]. I. Doymaz, “Convective air drying characteristics of thin layer carrots,” J. Food Eng., 2004.

[73]. R. B. Bird, W. E. Stewart, and E. N. Lightfoot, Transport Phenomena, 2nd Edition, 2 edition. New York: Wiley, 2001.

[74]. Tomas Jurena, “Numerical modelling of grate combustion,” Brno University of Technology, Brno, 2012.

[75]. M. R. Assari, H. Basirat Tabrizi, and M. Saffar-Avval, “Numerical simulation of fluid bed drying based on two-fluid model and experimental validation,” Appl. Therm. Eng., vol. 27, no. 2–3, pp. 422–429, Feb. 2007.

[76]. T. Gulati and A. K. Datta, “Mechanistic understanding of case-hardening and texture development during drying of food materials,” J. Food Eng., vol. 166, pp. 119–138, Dec. 2015.

[77]. Hrvoje Jasak, “Error Analysis and Estimation for the Finite Volume Mehtod with Applications to Fluid Flows,” Imperial College of Science, Technology and Medicine, 1996.

[78]. H. K. Dass, Advanced Engineering Mathematics. New Delhi: S Chand & Co Ltd, 2007.

[79]. Dhall and A. K. Datta, “Transport in deformable food materials: A poromechanics approach,” Chem. Eng. Sci., vol. 66, no. 24, pp. 6482–6497, Dec. 2011.

[80]. Mendis, ARL, Amarasinghe, ADUS, Narayana, M, “Numerical simulation of the moisture diffusion in copra drying process”, Moratuwa Engineering Research Conference (MERCon), pp.192-197, 2016.

[81]. R. Thuwapanichayanan, S. Prachayawarakorn, and J. Kunwisawa, “LWT - Food Science and Technology Determination of effective moisture diffusivity

and assessment of quality attributes of banana slices during drying," LWT - Food Sci. Technol., vol. 44, no. 6, pp. 1502–1510, 2011.

[82]. G. Bohm and G. Zech, "Comparison of experimental data to Monte Carlo simulation—Parameter estimation and goodness-of-fit testing with weighted events," Nucl. Instruments Methods Phys. Res. Sect. A Accel. Spectrometers, Detect. Assoc. Equip., vol. 691, pp. 171–177, Nov. 2012.

[83]. A. Maydeu-Olivares and C. García-Forero, International Encyclopedia of Education. Elsevier, 2010.

[84]. K. M. Ramachandran and C. P. Tsokos, Mathematical Statistics with Applications in R. Elsevier, 2015.

[85]. C. Ratti, "Shrinkage during drying of foodstuffs," J. Food Eng., vol. 23, no. 1, pp. 91–105, Jan. 1994.

[86]. M. S. Hatamipour and D. Mowla, "Shrinkage of carrots during drying in an inert medium fluidized bed," J. Food Eng., 2002.

[87]. L. Mayor and A. M. Sereno, "Modelling shrinkage during convective drying of food materials: A review," J. Food Eng., 2004.

[88]. P. Kaushal and H. K. Sharma, "Osmo-convective dehydration kinetics of jackfruit (Artocarpus heterophyllus)," J. SAUDI Soc. Agric. Sci., 2014.

[89]. J. A. K. M. Fernando and A. D. U. S. Amarasinghe, "Drying kinetics and mathematical modeling of hot air drying of coconut coir pith," Springerplus.

[90]. H. O. Menges and C. Ertekin, "Mathematical modeling of thin layer drying of Golden apples," J. Food Eng., 2006.

[91]. J. Wisniak and A. Polishuk, "Analysis of residuals a useful tool for phase equilibrium data analysis," Fluid Phase Equilib., vol. 164, pp. 61–82, 1999.

Appendix A: Publications

1. A.R.L. Mendis, A.D.U.S. Amarasinghe and M. Narayana “Numerical modelling of copra drying” (Journal paper in preperation).
2. A. R. L. Mendis, A. D. U. S. Amarasinghe, and M. Narayana, “Particle modelling for convective drying of copra,” in 2017 Moratuwa Engineering Research Conference (MERCon), 2017, pp. 7–12.
   DOI: 10.1109/MERCon.2017.7980447.
3. A. R. L. Mendis, A. D. U. S. Amarasinghe, and M. Narayana, “Numerical Simulation of the Moisture Diffusion in Copra Drying Process,” in 2016 Moratuwa Engineering Research Conference (MERCon), 2016, pp. 192–197.
   DOI: 10.1109/MERCon.2016.7480138.

Appendix B: OpenFOAM Solver Code

```
/*---------------------------------------------------------------------------*\
  =========                 |
  \\      /  F ield         | OpenFOAM: The Open Source CFD Toolbox
   \\    /   O peration     |
    \\  /    A nd           | Copyright (C) 2011-2013 OpenFOAM Foundation
     \\/     M anipulation  |
-------------------------------------------------------------------------------
License
    This file is part of OpenFOAM.

    OpenFOAM is free software: you can redistribute it and/or modify it
    under the terms of the GNU General Public License as published by
    the Free Software Foundation, either version 3 of the License, or
    (at your option) any later version.

    OpenFOAM is distributed in the hope that it will be useful, but WITHOUT
    ANY WARRANTY; without even the implied warranty of MERCHANTABILITY or
    FITNESS FOR A PARTICULAR PURPOSE.  See the GNU General Public License
    for more details.

    You should have received a copy of the GNU General Public License
    along with OpenFOAM.  If not, see <http://www.gnu.org/licenses/>.

Application
    icoFoam

Description
    Transient solver for incompressible, laminar flow of Newtonian fluids.

\*---------------------------------------------------------------------------*/

#include "fvCFD.H"

// * * * * * * * * * * * * * * * * * * * * * * * * * * * * * * * * * * * * * //
```

```
int main(int argc, char *argv[])
{
    #include "setRootCase.H"

    #include "createTime.H"
    #include "createMesh.H"
    #include "createFields.H"


    // * * * * * * * * * * * * * * * * * * * * * * * * * * * * * * * * * * * * //

    Info<< "\nStarting time loop\n" << endl;

//scalar I = 0.0001;
dimensionedScalar a
(
"a",
dimensionSet(1,-3,-1,0,0,0,0),
scalar(1)
);
dimensionedScalar d
(
"d",
dimensionSet(0,2,-1,0,0,0,0),
scalar(1)
);
dimensionedScalar t
(
"t",
dimensionSet(1,-1,-3,0,0,0,0),
scalar(1)
);
    while (runTime.loop())
    {
        Info<< "Time = " << runTime.timeName() << nl << endl;
//for liquid water

Mexp=(Mexpa*exp(Mexpb*V))+(Mexpc*exp(Mexpd*V));//(52.52*exp(-0.0001576*V))+(27.45*exp(-0.00002*V));//
```

```
//volScalarField Mt
//     (
//      "Mt",
//       TotalMc
//     );
for (int i=0; i<2; i++)//sqrt(pow((Mt-Mexp),2))>I
{

        fvScalarMatrix WEqn
        (
                fvm::ddt(W)
                -fvm::laplacian(D, W)
        );

        solve(WEqn == -k*(W-0.028)*a/(rhow));//WEqn.solve();
por=1-((1-0.8)*(1-W)/(1-iw));
MC=rhow*W*100/((1-por)*rhos);
TotalMC=(100/(rhos*dvol*(1-porosity)))*fvc::domainIntegrate(rhow*((W*pos(W))+(0*neg(W))));
volScalarField condition
     (
      "condition",
       (TotalMC-Mexp)*pos(TotalMC-Mexp)+(TotalMC-Mexp)*(-1)*neg(TotalMC-Mexp)//sqrt(pow((TotalMC-Mexp),2))
     );
//condition.write();
//Mexp.write();
if (condition>error)
{
i=0;
D=((D+Dmax)*pos(TotalMC-Mexp)/2)+((D+Dmin)*neg(TotalMC-Mexp)/2);
}
else
{
i=1;
//D=D;
}

}
V=V+0.05;
```

```
(
    transportProperties.lookup("dw")
);
dimensionedScalar dv
(
    transportProperties.lookup("dv")
);
dimensionedScalar dvol
(
    transportProperties.lookup("dvol")
);
dimensionedScalar Tt
(
    transportProperties.lookup("Tt")
);
dimensionedScalar da
(
    transportProperties.lookup("da")
);
dimensionedScalar db
(
    transportProperties.lookup("db")
);
dimensionedScalar k
(
    transportProperties.lookup("k")
);
dimensionedScalar DT
(
    transportProperties.lookup("DT")
);
dimensionedScalar Dmax
(
    transportProperties.lookup("Dmax")
);
dimensionedScalar Dmin
(
    transportProperties.lookup("Dmin")
);
 (
     transportProperties.lookup("rhos")
 );
 dimensionedScalar rhog
 (
     transportProperties.lookup("rhog")
 );
 dimensionedScalar porosity
 (
     transportProperties.lookup("porosity")
 );
 dimensionedScalar dw
```

```
dimensionedScalar Dmin
(
    transportProperties.lookup("Dmin")
);
dimensionedScalar cp
(
    transportProperties.lookup("cp")
);
dimensionedScalar Mexpa
(
    transportProperties.lookup("Mexpa")
);
dimensionedScalar Mexpb
(
    transportProperties.lookup("Mexpb")
);
dimensionedScalar Mexpc
(
    transportProperties.lookup("Mexpc")
);
dimensionedScalar Mexpd
(
    transportProperties.lookup("Mexpd")
);
dimensionedScalar iw
(
    transportProperties.lookup("iw")
);


 Info<< "Reading field W\n" << endl;
 volScalarField W
 (
     IOobject
     (
         "W",
         runTime.timeName(),
         mesh,
         IOobject::MUST_READ,
         IOobject::AUTO_WRITE
     ),
     mesh
 );
 Info<< "Reading field V\n" << endl;
 volScalarField V
 (
     IOobject
     (
         "V",
         runTime.timeName(),
         mesh,
         IOobject::MUST_READ,
         IOobject::AUTO_WRITE
     ),
     mesh
 );
 Info<< "Reading field D\n" << endl;
 volScalarField D
 (
     IOobject
     (
         "D",
         runTime.timeName(),
         mesh,
         IOobject::MUST_READ,
         IOobject::AUTO_WRITE
     ),
```

```
    );
    Info<< "Reading field MC\n" << endl;
    volScalarField MC
    (
        IOobject
        (
            "MC",
            runTime.timeName(),
            mesh,
            IOobject::MUST_READ,
            IOobject::AUTO_WRITE
        ),
        mesh
    );
    Info<< "Reading field TotalMC\n" << endl;
    volScalarField TotalMC
    (
        IOobject
        (
            "TotalMC",
            runTime.timeName(),
            mesh,
            IOobject::MUST_READ,
            IOobject::AUTO_WRITE
        ),
        mesh
    );
    Info<< "Reading field Mexp\n" << endl;
    volScalarField Mexp
    (
        IOobject
        (
            "Mexp",
            runTime.timeName(),
            mesh,
            IOobject::MUST_READ,
            IOobject::AUTO_WRITE
        ),


    mesh
);
Info<< "Reading field error\n" << endl;
volScalarField error
(
    IOobject
    (
        "error",
        runTime.timeName(),
        mesh,
        IOobject::MUST_READ,
        IOobject::AUTO_WRITE
    ),
    mesh
);

Info<< "Reading field por\n" << endl;
volScalarField por
(
    IOobject
    (
        "por",
        runTime.timeName(),
        mesh,
        IOobject::MUST_READ,
        IOobject::AUTO_WRITE
    ),
    mesh
);
```

```
Info<< "Reading field T\n" << endl;
volScalarField T
(
    IOobject
    (
        "T",
        runTime.timeName(),
        mesh,
        IOobject::MUST_READ,
        IOobject::AUTO_WRITE
    ),
    mesh
);
```